

Phospholipase D α 1 and Phosphatidic Acid Regulate NADPH Oxidase Activity and Production of Reactive Oxygen Species in ABA-Mediated Stomatal Closure in *Arabidopsis*

Yanyan Zhang,^{a,1,2} Huiying Zhu,^{a,1} Qun Zhang,^{a,1} Maoyin Li,^{b,c,1} Min Yan,^a Rong Wang,^a Liling Wang,^a Ruth Welti,^d Wenhua Zhang,^{a,3} and Xuemin Wang^{b,c}

^aCollege of Life Sciences, State Key Laboratory of Crop Genetics and Germplasm Enhancement, Nanjing Agricultural University, Nanjing 210095, People's Republic of China

^bDepartment of Biology, University of Missouri, St. Louis, Missouri 63121

^cDonald Danforth Plant Science Center, St. Louis, Missouri 63132

^dKansas Lipidomics Research Center, Division of Biology, Kansas State University, Manhattan, Kansas 66506

We determined the role of Phospholipase D α 1 (PLD α 1) and its lipid product phosphatidic acid (PA) in abscisic acid (ABA)-induced production of reactive oxygen species (ROS) in *Arabidopsis thaliana* guard cells. The *pld α 1* mutant failed to produce ROS in guard cells in response to ABA. ABA stimulated NADPH oxidase activity in wild-type guard cells but not in *pld α 1* cells, whereas PA stimulated NADPH oxidase activity in both genotypes. PA bound to recombinant *Arabidopsis* NADPH oxidase RbohD (respiratory burst oxidase homolog D) and RbohF. The PA binding motifs were identified, and mutation of the Arg residues 149, 150, 156, and 157 in RbohD resulted in the loss of PA binding and the loss of PA activation of RbohD. The *rbohD* mutant expressing non-PA-binding RbohD was compromised in ABA-mediated ROS production and stomatal closure. Furthermore, ABA-induced production of nitric oxide (NO) was impaired in *pld α 1* guard cells. Disruption of PA binding to ABI1 protein phosphatase 2C did not affect ABA-induced production of ROS or NO, but the PA-ABI1 interaction was required for stomatal closure induced by ABA, H₂O₂, or NO. Thus, PA is as a central lipid signaling molecule that links different components in the ABA signaling network in guard cells.

INTRODUCTION

The plant hormone abscisic acid (ABA) participates in diverse physiological processes, such as stomatal movement, seed dormancy and germination, vegetative growth, and response to abiotic and biotic stresses (Schroeder et al., 2001; Finkelstein et al., 2002; Assmann, 2003; Xiong and Zhu, 2003; Hirayama and Shinozaki, 2007). Under drought stress, ABA promotes stomatal closing and inhibits stomatal opening, thereby reducing transpiration and water loss. Using forward and reverse genetics and cellular, biochemical, and molecular approaches, a number of components in ABA signal transduction have been characterized, including G proteins, protein kinases/phosphatases, transcriptional factors, receptors, and enzymes involved in producing reactive oxygen species (ROS), such as O₂⁻ and

H₂O₂ (Gosti et al., 1999; Merlot et al., 2001; Wang et al., 2001; Himmelbach et al., 2002; Mishra et al., 2006; Shen et al., 2006; Liu et al., 2007; Nilson and Assmann, 2007; Ma et al., 2009; Pandey et al., 2009; Park et al., 2009). In addition, lipid mediators generated by phospholipase D (PLD), phospholipase C (PLC), and sphingosine kinase have been identified as integral parts of the complex signaling cascades in the ABA response (Fan et al., 2004; Zhang et al., 2005; Wang et al., 2006). Recent studies show that PLD and its lipid product phosphatidic acid (PA) interact with a G protein and protein phosphatase to mediate the ABA response in guard cells. Abrogation of *Phospholipase D α 1* (*PLD α 1*) renders *Arabidopsis thaliana* insensitive to ABA in stomatal closure and leads to more water loss than in wild-type plants (Zhang et al., 2004), whereas overexpression of *PLD α 1* results in less water loss (Sang et al., 2001b). PLD α 1-produced PA binds to the ABI1 protein phosphatase 2C, a negative regulator of ABA action. This interaction inhibits the function of ABI1 by inhibiting its phosphatase activity and tethers it to the plasma membrane. Membrane tethering is thought to prevent the interaction of ABI1 with the transcription factor ATHB6 (Zhang et al., 2004). On ABA inhibition of stomatal opening, PLD α 1 binds to GPA1 (α -subunit of heterotrimeric G protein) and regulates its function by promoting the conversion of GTP-bound G α to a GDP-bound G α , thus producing PA that acts upstream of G α to inhibit stomatal opening (Mishra et al., 2006).

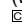
PLD and PA are both implicated in ROS production. The depletion of *PLD α 1* in *Arabidopsis* decreases ROS production in

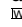
¹ These authors contributed equally to this work.

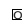
² Current address: State Key Laboratory of Genetic Engineering, Institute of Plant Biology, School of Life Sciences, Fudan University, Shanghai 200433, People's Republic of China.

³ Address correspondence to whzhang@njau.edu.cn.

The author responsible for distribution of materials integral to the findings presented in this article in accordance with the policy described in the Instructions for Authors (www.plantcell.org) is: Wenhua Zhang (whzhang@njau.edu.cn).

 Some figures in this article are displayed in color online but in black and white in the print edition.

 Online version contains Web-only data.

 Open access articles can be viewed online without a subscription.

www.plantcell.org/cgi/doi/10.1105/tpc.108.062992

leaves, and addition of PA results in recovery of ROS production in *pldα1* mutants (Sang et al., 2001a). In response to an avirulent elicitor in tomato (*Solanum lycopersicum*), PA induces an oxidative burst (de Jong et al., 2004). PA induces leaf cell death in *Arabidopsis* by activating small G protein ROP2-mediated pathway of ROS generation (Park et al., 2004). NADPH oxidases are the source of ROS produced in ABA response and other processes, including pathogen recognition and root hair growth (Torres et al., 2002; Foreman et al., 2003; Kwak et al., 2003; Torres and Dangl, 2005). Plant NADPH oxidases, termed respiratory burst oxidase homologs (Rboh), are homologs of the mammalian NADPH oxidase catalytic subunit gp91^{phox}. Different *Rboh* genes have been isolated from rice (*Oryza sativa*), *Arabidopsis*, tomato (*Solanum lycopersicum*), tobacco (*Nicotiana tabacum*), and potato (*Solanum tuberosum*) (Torres and Dangl, 2005). *Arabidopsis* has 10 *Rboh* genes with diversified functions. *Arabidopsis RbohC* is required for the root hair development (Foreman et al., 2003), whereas *RbohD* and *RbohF* are involved in pathogen recognition and ABA-induced stomatal closure (Torres et al., 2002; Kwak et al., 2003; Bright et al., 2006). In *Nicotiana benthamiana*, *RbohA* and *RbohB* participate in ROS accumulation and viral resistance (Yoshioka et al., 2003).

In phagocytic cells, NADPH oxidase contains plasma membrane-bound cytochrome *b₅₅₈* (gp91^{phox} and p22^{phox}) and cytosolic regulatory proteins, including p67^{phox}, p47^{phox}, p40^{phox}, and small GTP binding protein Rac (Babior, 2004). Activation of the oxidase requires translocation of the cytosolic subunits to membrane-bound gp91^{phox} and p22^{phox} complex, and the p47^{phox} subunit is regarded as a key regulator in the translocation (Karathanassis et al., 2002). During cell stimulation, p47^{phox} is recruited to the membrane via SH3-mediated interaction with p22^{phox} and Phox homology (PX)-mediated binding to phosphoinositides (PtdInsP₂) and PA (Karathanassis et al., 2002; Ago et al., 2003). On the other hand, the membrane recruitment of p67^{phox} is mediated via its binding to p47^{phox} (Heyworth et al., 1991; Kami et al., 2002), whereas Rac is independently tethered to the membrane (Heyworth et al., 1994). These cytosolic regulatory proteins translocate to the plasma membrane to form an active enzyme complex capable of producing superoxide.

Homologs of the cytosolic regulator small GTPase Rac of mammalian NADPH oxidase are found in plants (Groom et al., 1996; Keller et al., 1998; Torres et al., 1998; Kawasaki et al., 1999; Wong et al., 2007), but no homologs of other regulatory components of mammalian NADPH oxidase, namely, p22^{phox}, p67^{phox}, p47^{phox}, and p40^{phox}, are found in the *Arabidopsis* genome (Torres and Dangl, 2005). In contrast with mammalian NADPH oxidases, plant Rboh proteins possess an extended N terminus with two Ca²⁺ binding EF-hand motifs. Using a heterologous expression system, a Ca²⁺ increase in the cytosol was found to be necessary for stimulating *Arabidopsis RbohD*. This stimulation requires a conformational change in the EF region, which is caused by Ca²⁺ binding (Ogasawara et al., 2008). Ca²⁺ may also regulate Rboh activity and ROS generation by phosphorylation mediated by calcium-dependent protein kinases (CDPKs) (Kobayashi et al., 2007; Ogasawara et al., 2008). Early genetic evidence pointed to involvement of the small GTPase in the regulation of ROS in plants (Ono et al., 2001; Schultheiss et al., 2002; Suharsono et al., 2002; Morel et al., 2004). The direct

binding of rice Rac1 to the N terminus of rice RbohB was characterized recently (Wong et al., 2007). Rac-Rboh binding leads to an increase in ROS, thus inducing cytosolic Ca²⁺ accumulation, whereas an increase in cytosolic Ca²⁺ inhibits the Rac-Rboh interaction and reduces ROS production (Wong et al., 2007). Asai et al. (2008) reported that MAPK cascades regulate the expression of *N. benthamiana RbohB* and oxidative burst. However, compared to mammalian NADPH oxidase, much less is known about the regulatory mechanisms of plant Rboh. Specifically, it is unknown whether membrane factors, such as lipid mediators, regulate Rboh activity.

Arabidopsis RbohD and *RbohF* are located in the plasma membrane (Torres and Dangl, 2005, and references within), and *RbohD* and *RbohF* are expressed in *Arabidopsis* guard cells (Kwak et al., 2003). *pldα1* and *rbohD/F* mutants show similar phenotypes; they are both insensitive to ABA-induced stomatal closure (Kwak et al., 2003; Zhang et al., 2004). PA stimulates ROS production in *Arabidopsis* leaves (Sang et al., 2001a). In light of these observations, this study was undertaken to address whether and how PLD and PA regulate ABA-mediated ROS generation in guard cells. The results show that PLDα1 is required for the ABA activation of NADPH oxidase and the production of ROS and that PLDα1-derived PA interacts directly with RbohD. In addition, the data indicate that the production and action of NO are downstream of the PLDα1-mediated production of PA and ROS. The interaction between PA and ABI1 is not required for the ABA-induced production of ROS and NO but is important for mediating the ROS effect on stomatal closure.

RESULTS

Loss of PLDα1 Leads to a Decrease in ABA-Mediated ROS Production in Guard Cells

The *PLDα1*-null *Arabidopsis* mutant, *pldα1*, which contains a T-DNA insertion 1027 nucleotides downstream of the initiation codon, was insensitive to ABA-induced stomatal closure (Zhang et al., 2004; Mishra et al., 2006). The ABA response of the mutant was restored to that of the wild type after *pldα1* was complemented with the native *PLDα1* gene, verifying that the loss of *PLDα1* is responsible for the defect in ABA response (Mishra et al., 2006). To further determine the cellular role of *PLDα1* in the regulation of stomatal closure, we compared ROS production in *pldα1* and wild-type guard cells using the ROS-sensitive, cell-permeable, fluorescent dye, 2',7'-dichlorofluorescein diacetate (H₂DCFDA) (Pei et al., 2000). H₂DCFDA diffuses through the cell membrane and is hydrolyzed by intracellular esterases to form nonfluorescent H₂DCF, which is oxidized to fluorescent DCF by ROS (Wang and Joseph, 1999). H₂DCFDA is an effective dye for measuring ROS in our system because ABA-induced DCF fluorescence was shown to be inhibited by a suicide substrate inhibitor of NADPH oxidases, diphenylene iodonium (DPI). As a positive control, the superoxide donor phenazine methosulfate (5 μM) resulted in an increase in DCF fluorescence (see Supplemental Figure 1 online).

Without ABA treatment, wild-type and *pldα1* guard cells exhibited similar basal staining of ROS. Treatment of epidermal

strips with 50 μM ABA induced a rapid (within 5 min) increase in ROS levels, as indicated by the change in fluorescent intensity compared with the tissue not exposed to ABA treatment (Figure 1A). Approximately a 38% increase in ROS level occurred in wild-type guard cells after the ABA treatment. However, no increase in ROS was observed in *pld α 1* guard cells after ABA treatment for up to 10 min (Figures 1A and 1B). ABA was dissolved in ethanol (0.1%, v/v), and this level of ethanol alone had no effect on ROS generation, *RAB18* expression, PLD α activity, and stomatal closure (see Supplemental Figure 2 online). The effect of ABA on ROS increase in the wild type and *pld α 1* was verified by measuring the total H_2O_2 content in leaves with an Amplex red hydrogen peroxide/peroxidase assay kit (Molecular Probes) (see Supplemental Figure 3A online). The results indicate that PLD α 1 is required for ABA-mediated ROS production in guard cells.

To determine whether the loss of *PLD α 1* affects the ROS response in guard cells, we tested the effect of H_2O_2 on stomatal movement in wild-type and *pld α 1* leaves. H_2O_2 induced stomatal closure in both the wild type and *pld α 1* (Figure 1C) in a dosage-

dependent manner (see Supplemental Figure 3B online). By contrast, ABA induced stomatal closure in the wild type, but not *pld α 1* (Figure 1C). Thus, the loss of *PLD α 1* impairs the production of ROS but does not affect the stomatal response to ROS, suggesting that PLD α 1 acts upstream of ROS and may regulate its production in the ABA signaling pathway.

PLD α 1 Mediates ABA-Induced ROS Production via NADPH Oxidase

To examine how PLD α 1 affects ROS production, we investigated the effect of PLD α 1 and PA on NADPH oxidase activity in wild-type and *pld α 1* plants subjected to ABA treatment. NADPH oxidase has been reported to be an important source of ROS production in ABA signaling in *Arabidopsis* (Kwak et al., 2003; Suhita et al., 2004). When the epidermal strips were pretreated with the NADPH oxidase inhibitor DPI, the ABA-induced stomatal closure was inhibited in the wild type (Figure 1D), suggesting that activation of NADPH oxidase is required for ABA-induced stomatal closure. The treatment of DPI did not alter the stomatal

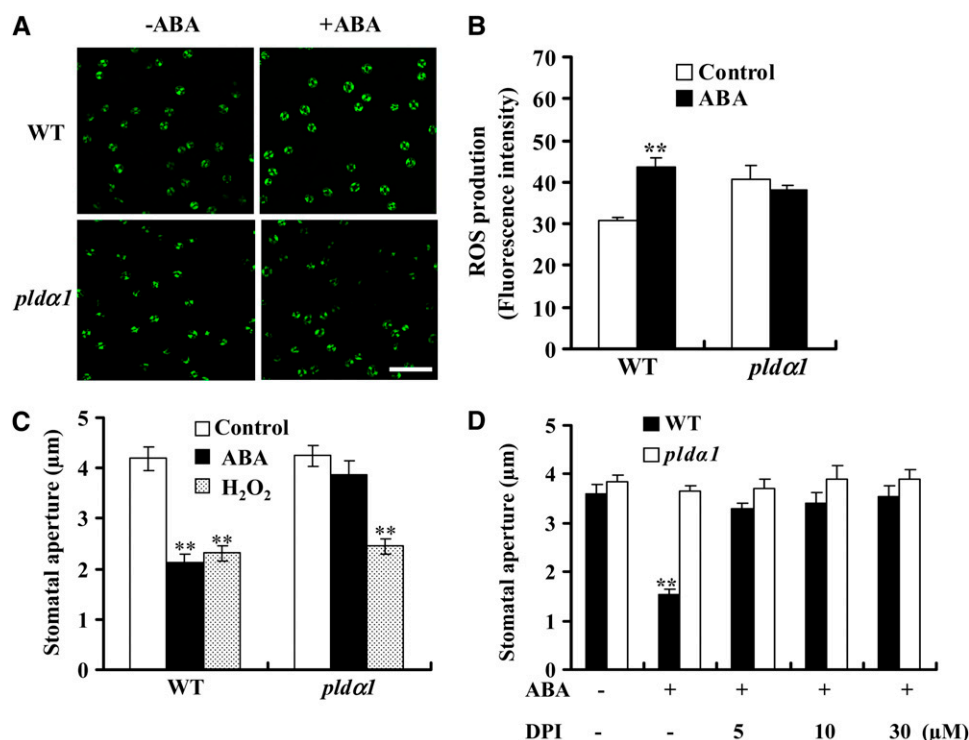


Figure 1. PLD α 1 Mediates ABA-Induced ROS Production and Stomatal Closure.

(A) Representative images of ROS production indicated by fluorescent dye DCF. Epidermal peels were loaded with H_2DCFDA for 10 min before adding 50 μM ABA. Photomicrographs were taken 5 min after ABA addition. Bar = 100 μm .

(B) Quantification of ROS production in guard cells of the wild type and *pld α 1* following ABA treatment. Confocal planes were quantified as mean pixel intensities. The data are means \pm SE from three independent experiments; $n = 50$ of each genotype per experiment.

(C) Applied H_2O_2 induces stomatal closure in the wild type and *pld α 1*. The data are means \pm SE from three independent experiments; $n = 60$ apertures each genotype per experiment.

(D) Effect of NADPH oxidase inhibitor DPI on ABA-induced stomatal closure. The epidermal peels were pretreated with DPI for 30 min before 50 μM ABA was added. The data are means \pm SE from three independent experiments; $n = 50$ apertures each genotype per experiment.

For all stomatal bioassays, at least three separate peels were observed for each treatment per genotype. Data were compared using Student's t test. Two asterisks in (B) to (D) indicate that the mean value is significantly different from that of the control ($P < 0.01$).

aperture of *pldα1*, presumably because NADPH oxidase activity in the mutant guard cells was not activated in response to ABA.

To determine whether PLD α 1 is involved in NADPH oxidase activation, we measured NADPH oxidase activity using guard cell protoplasts (GCPs) isolated from leaf epidermal strips. PLD α 1 protein was present in both mesophyll cell protoplasts (MCPs) and GCPs of the wild type, but not of *pldα1* (Figure 2A). Treatment of GCPs with 10 μ M ABA induced an increase in O $_2^-$ levels, measured as a reduction of tetrazolium dye (XTT) in the wild type compared with the control (0.02% ethanol only, v/v). ABA-induced O $_2^-$ generation declined sharply in *pldα1* GCPs (Figure 2B). These results suggest that PLD α 1 is involved in ABA-induced activation of NADPH oxidase and ROS production.

ABA Induces Different Changes in PA Species in the Wild Type and *pldα1*

We previously showed that PLD α 1 was activated in the ABA response and that phosphatidylcholine (PC) was hydrolyzed to PA in leaf protoplasts labeled with fluorescent PC (Zhang et al., 2004). To further characterize the PA change in response to ABA, we used electrospray ionization–tandem mass spectrometry (ESI-MS/MS) to analyze PA species in leaves. The level of total PA was lower in *pldα1* than in wild-type leaves, with or without ABA treatments (Figure 3A). ABA induced a transient increase in PA, with a maximum increase occurring at 10 min after ABA application to wild-type leaves. Total PA in *pldα1* leaves also increased after an application of ABA, which may result from activities of other PLDs and/or diacylglycerol kinases (DGKs). However, the amount of PA in the mutant after 10 min of ABA treatment was 2.4-fold lower than that in the wild type.

Analysis of PA molecular species revealed further distinguishable changes between wild-type and *pldα1* plants after ABA treatment (Figures 3B and 3C). The major molecular species of PAs in the wild type were 34:2 (16:0-18:2), 34:3 (16:0-18:3), 36:4 (18:2-18:2), 36:5 (18:2-18:3), and 36:6 (18:3-18:3) (Devaiah et al., 2006; Figure 3B). Although the basal levels of PA species 34:1 (16:0-18:1) and 36:3 (18:1-18:2) were very low, the level of these PAs dramatically increased 10 min after ABA application. In addition, 34:2, 34:3, and 36:6 PAs were significantly increased in wild-type leaves after ABA treatment for 10 min (Figure 3B). In comparison, in *pldα1*, the PA species induced by ABA were primarily 34:2, 34:3, 36:4, and 36:5 PAs (Figure 3C). In addition, the magnitude of increase in 34:2 PA at 10 min was lower in *pldα1* than in wild-type leaves. After a 10-min ABA treatment, the contents of 34:2, 34:3, 36:3, 36:4, 36:5, and 36:6 PAs in wild-type leaves were significantly higher than those in *pldα1* mutant leaves (Figure 3D). The results show that abrogation of PLD α 1 leads to changes in the amount, the magnitude, and molecular species of PA in response to ABA.

PA Binds to NADPH Oxidases

To investigate how PA affects NADPH oxidase function, we examined the potential interaction of PA with RbohD and RbohF, which are the major Rbohs in guard cells and are upregulated by ABA (Kwak et al., 2003). These Rbohs share about 49% identity

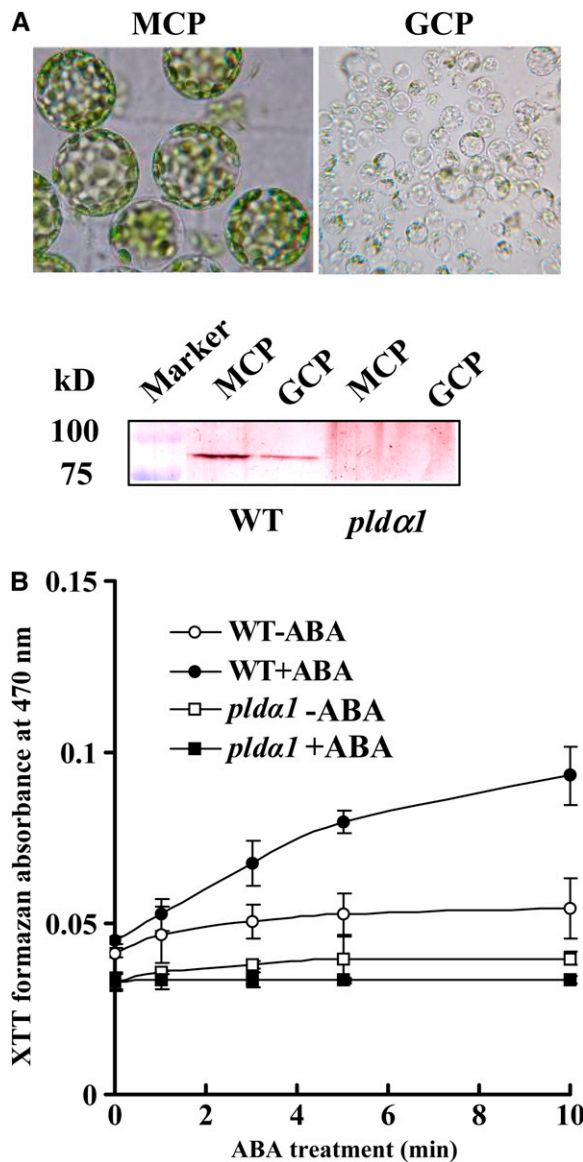


Figure 2. PLD α 1 and PA Mediate ABA-Enhanced NADPH Oxidase Activity and ROS Production.

(A) Isolated MCPs and GCPs (top panel); immunoblotting of PLD α 1 (bottom panel). Proteins from the wild type (MCPs, 26 μ g; GCPs, 15 μ g) and *pldα1* (MCPs, 30 μ g; GCPs, 22 μ g) were separated by 8% SDS-PAGE. PLD α 1 was made visible by alkaline phosphatase staining after blotting with PLD α antibody.

(B) ABA-induced O $_2^-$ production in the wild type and *pldα1* GCPs (4×10^4 protoplasts). GCPs were treated with 10 μ M (\pm) ABA dissolved in 0.02% (v/v) ethanol (+ABA) or 0.02% (v/v) ethanol only (–ABA). O $_2^-$ production was measured by the detection of XTT formazan using spectrophotometric analysis at A_{470} . Data are means \pm SE of three independent experiments.

in predicted amino acid sequences (see Supplemental Figure 4 online). RbohD and RbohF were expressed in *Escherichia coli* as His-tagged proteins using *RbohD* and *RbohF* cDNAs cloned from wild-type *Arabidopsis*. The isolated proteins were tested for lipid binding using a filter-binding assay. Compared with the

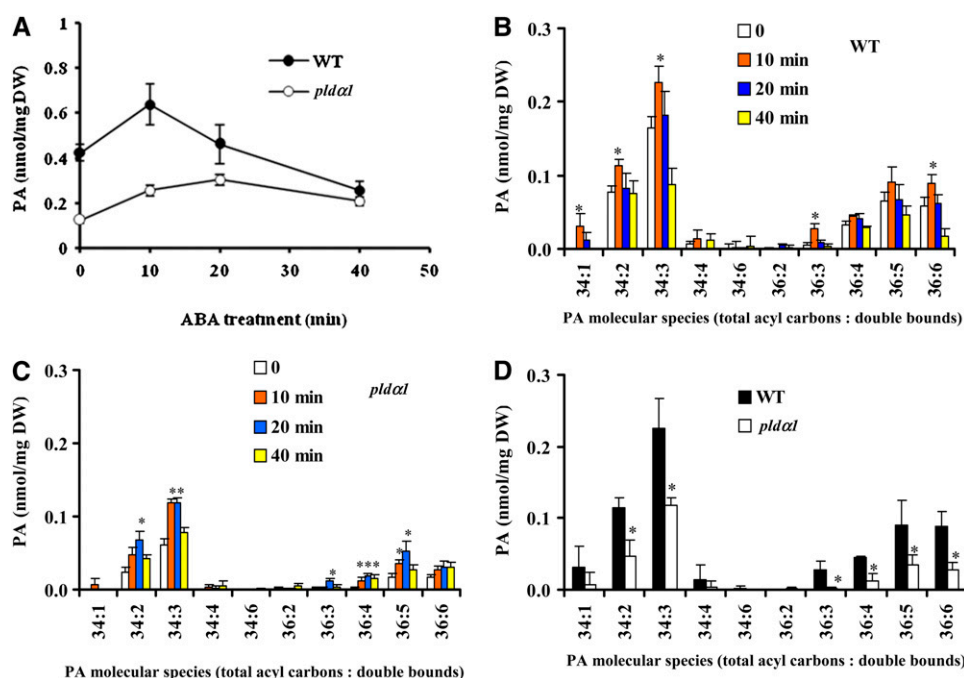


Figure 3. ABA-Induced Changes in PA Species in Arabidopsis Leaves.

(A) Change in total PA content in leaves after ABA treatment.

(B) and (C) ABA-induced changes in PA molecular species in the wild type (B) and *pldα1* (C).

(D) Comparison of PA molecular species in wild-type and *pldα1* leaves treated with ABA for 10 min.

Data in (A) to (D) are means \pm SE ($n = 4$ or 5). The asterisk in (B) and (C) indicates that the mean value is significantly higher than that of leaves not subjected to ABA treatment (0 time) ($P < 0.05$). The asterisk in (D) indicates that the mean value is significantly different from that of the wild type ($P < 0.05$).

empty vector control, both Rboh D and RbohF bound to PA from egg yolk, but not to PC, phosphatidylethanolamine, phosphatidylglycerol, phosphatidylinositol, phosphatylserine, or diacylglycerol (Figure 4A). PA binding to RbohD was stronger than binding to RbohF. RbohD and RbohF also bound to lysoPA, but more weakly than to PA. Phosphatidylinositol 3-phosphate [PtdIns(3)P], which is essential for ROS generation in the salt stress response (Leshem et al., 2007) and stomatal closure induced by ABA (Park et al., 2003), has been demonstrated to bind to mammalian NADPH oxidase subunit p40^{phox} (Kanai et al., 2001; Honbou et al., 2007). Therefore, we further investigated RbohD and RbohF binding to PtdIns(3)P, PtdIns(4)P, and PtdIns(3,4)P₂, and no lipid-RbohD (or -RbohF) binding was found (see Supplemental Figure 5 online). To investigate the specific interaction of PA with RbohD (or RbohF), we tested different PA species. Both RbohD and RbohF bound to dioleoyl PA (di18:1 PA), dilinoleoyl PA (di18:2 PA), palmitoyl-oleoyl PA (16:0-18:1 PA), palmitoyl-linoleoyl PA (16:0-18:2 PA), and stearoyl-linoleoyl PA (18:0-18:2 PA), but not to dipalmitoyl PA (di16:0 PA) or distearoyl PA (di18:0 PA). RbohD displayed stronger binding than did RbohF (Figure 4B). Because 16:0-18:2 PA is commercially available and is a PA species that is significantly increased by exposure to ABA in *Arabidopsis* leaves, we used 16:0-18:2 PA for functional analysis in further experiments.

The lipid-RbohD (-RbohF) interaction was further determined using an ELISA-based assay (Ghosh et al., 1996). 16:0-18:2 PA

was coated on microtiter plates and incubated with His-tagged RbohD or RbohF. Both RbohD and RbohF bound to PA in a dose-dependent manner, but the binding of RbohF was weaker than that of RbohD (Figure 4C). The results were consistent with those of filter binding experiments (Figure 4B). Increases in RbohD and RbohF concentrations had no effect on PC binding capacity (Figure 4D). These results suggest that RbohD and RbohF specifically bind to PA.

A Specific PA Species Activates NADPH Oxidase

To determine whether PLD α 1-derived PA affects NADPH oxidase activity, we tested the effects of 16:0-18:2 PA on ROS generation in GCPs. Treatment of MCPs with 16:0-18:2 PA resulted in the activation of NADPH oxidase activity in the wild type in a dose-dependent manner, reaching a maximum at 1 μ M. By contrast, 16:0-18:2 PC had no stimulatory effect (see Supplemental Figure 6 online). We then determined the effects of different lipids on NADPH oxidase activity in wild-type and *pldα1* GCPs. 16:0-18:2 PA stimulated NADPH oxidase activity in both the wild type and *pldα1*, whereas 16:0-18:2 PC or LysoPA did not affect the activity significantly (Figure 5A). Di16:0 PA had no effect on ROS production in GCPs or on stomatal closure (see Supplemental Figures 7A and 7B online).

We next isolated plasma membrane vesicles from leaves. Application of 16:0-18:2 PA (1 μ M) to vesicles stimulated plasma

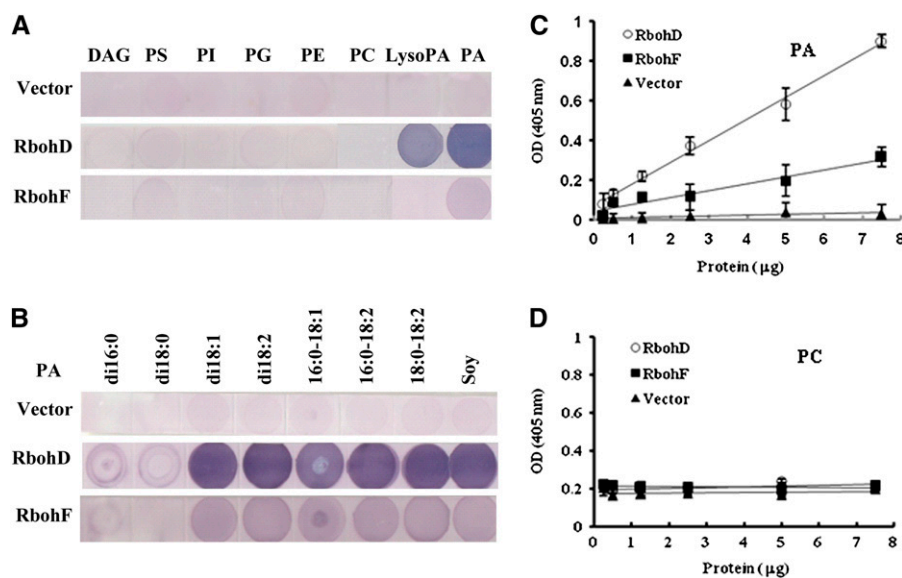


Figure 4. PA Binds to RbohD and RbohF Proteins.

(A) Lipid binding specificity of RbohD and RbohF proteins on filters. Lipids (10 μ g) were spotted onto nitrocellulose and incubated with purified RbohD and RbohF expressed in *E. coli*. Equal amounts of RbohD and RbohF protein were used. The protein bound to lipids was visualized by immunoblotting. Lipids from egg yolk were used. DAG, diacylglycerol; PS, phosphatidylserine; PI, phosphatidylinositol; PG, phosphatidylglycerol; PE, phosphatidylethanolamine; PC, phosphatidylcholine; LysoPA, oleoyl lyso PA.

(B) Different PA species bind to RbohD and RbohF proteins on filters. PA species on filters include dipalmitoyl PA (di16:0 PA), distearoyl PA (di18:0 PA), dioleoyl PA (di18:1 PA), dilinoleoyl PA (di18:2 PA), palmitoyl-oleoyl PA (16:0-18:1 PA), palmitoyl-linoleoyl PA (16:0-18:2 PA), stearoyl-linoleoyl PA (18:0-18:2 PA), and natural PA (from soy).

(C) Binding of RbohD and RbohF proteins to 16:0-18:2 PA by ELISA assay.

(D) Binding of RbohD and RbohF proteins to 16:0-18:2 PC by ELISA assay.

The data in **(C)** and **(D)** are means \pm SE of three replicates.

[See online article for color version of this figure.]

membrane-associated NADPH oxidase activity, whereas the same concentration of PC did not stimulate the activity (Figure 5B). Unlike the case in GCPs (Figure 5A), ABA had no stimulation on NADPH oxidase activity associated with the plasma membrane. These results suggest that ABA does not directly stimulate the activity of NADPH oxidase or PLD but acts through other intracellular factors.

Identification of the PA Binding Region and Sites in Rbohs

To identify the protein region involved in PA binding, serial deletion mutants of RbohD and RbohF were generated and expressed in *E. coli*. As shown in Figure 6A, all plant Rbohs have an N-terminal extension with two EF-hand motifs, six transmembrane domains, and flavin adenine dinucleotide and NADPH binding motifs at the C terminus (Torres and Dangl, 2005). Deletion of the amino acid residue 331 to the C terminus did not affect PA binding of RbohD, indicating that the PA binding region resides in the N-terminal 330-amino acid residues. However, the peptide consisting of only the first 100 amino acids displayed no PA binding (Figure 6B), suggesting that the PA binding motif resides in amino acid residues 101 to 330 of RbohD. For RbohF, the PA binding motif was mapped to amino acid residues 104 to 341 (Figure 6C).

The PA-RbohD (or -RbohF) interaction was further examined by a liposome binding assay. Purified N-terminal fragments of RbohD (residues 1 to 100 and 1 to 330) and of RbohF (residues 1 to 104 and 1 to 341) were incubated with lipid vesicles comprised of PC and PA at a ratio of 3:1 or PC only. The vesicles were then pelleted and examined by immunoblotting to determine the amount of RbohD (or RbohF) fragments associated with liposomes. As shown in Figure 6D, RbohD330 (residues 1 to 330) and RbohF341 (residues 1 to 341) bound to the PA-containing vesicles but not to the PC-only vesicles (Figure 6D). When the same amount of each fragment was incubated with PC:PA vesicles, band intensity indicated that more RbohD330 than RbohF341 was present in the pelleted liposomes (Figure 6D). For RbohD100 and RbohF104, significantly less binding was observed in vesicles comprised of either PC (for D100 and F104) or PC/PA (F104). The results confirm that the PA binding region resides in amino acid residues 101 to 330 (RbohD) and 105 to 341 (RbohF).

Further deletions were conducted to map the PA binding motif. The RbohD140 fragment (residues 1 to 140) showed no PA binding ability, and RbohD150 had less PA binding activity than did the full-length protein, whereas RbohD160 bound to PA with a similar affinity as did the full-length RbohD (Figures 6B and 7A). The results indicate that amino acid residues 140 to 160 are

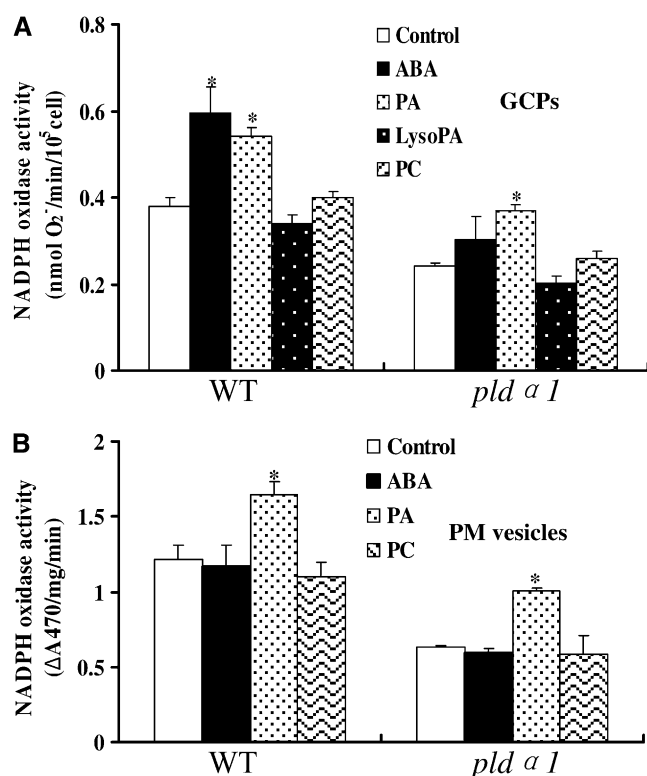


Figure 5. PA Activates NADPH Oxidase Activity in GCPs and the Plasma Membrane.

(A) The effect of PA on NADPH oxidase activity in GCPs. GCPs were incubated with XTT dye together with 1 μ M 16:0-18:2 PA, 16:0-18:2 PC, or LysoPA or 10 μ M ABA at 25°C for 10 min. After centrifugation, the supernatant was used for spectrophotometric analysis of XTT formazan production at A_{470} . The NADPH activity calculation is described in Methods.

(B) The effect of PA on NADPH oxidase activity in the plasma membrane. Plasma membrane vesicles (3 to 6 μ g protein) were incubated with XTT, together with 1 μ M 16:0-18:2 PA, 16:0-18:2 PC, or 10 μ M ABA at 25°C for 10 min. The reaction solution was used for spectrophotometric analysis of XTT formazan production at A_{470} . NADPH oxidase activity was expressed as ΔA_{470} per mg protein per min (ΔA_{470} represents the difference of XTT formazan absorbance at 470 nm in the presence and absence of superoxide dismutase [SOD]).

The data are means \pm SE of three independent experiments. The asterisk in **(A)** and **(B)** indicates that the mean value is significantly different from that of the control ($P < 0.05$).

required for PA binding. The potential PA binding motif of RbohD is rich in the basic residue Arg (Supplemental Figure 4 online). Basic residues are usually involved in PA binding, but a consensus amino acid sequence has yet to be identified as a common PA binding motif in animals and/or plants (Wang et al., 2006). To determine whether the amino acid residues are involved in PA binding, several Arg residues were mutated to Ala or Gly (Figure 7B). Single mutations R141A and R160A did not affect PA binding to RbohD compared with the PA binding fragment RbohD160. The double mutation R(144,145)A had no effect on PA binding (Figure 7B). Another double mutation R(156,157)A

slightly decreased PA binding compared to RbohD160. However, the quadruple mutation R(149,150,156,157)A caused RbohD160 to lose the ability to bind PA. The change of R149 and R150 to Gly also resulted in an obvious decrease in RbohD160 binding to PA (Figure 7B). The data suggest that R(149,150,156,157) are important residues in the binding of RbohD to PA.

We next determined the effect of these basic amino acid residues on the interaction between PA and RbohD (RbohF) in guard cell protoplasts. We expressed the PA binding fragment RbohD160 (1 to 160 amino acids) tagged with HA in the *RbohD*-null mutant (SALK-120299, named *rbohD*; Figure 8A) GCPs. The protein levels of RbohD160 and its quadruple mutant [R(149,150,156,157)A] were similar, as measured by immunoblotting (Figure 8B, top panel). The protoplasts expressing these proteins were labeled with fluorescent 12[[7-nitro-2-1,3-benzoxadiazol-4-yl) amino] dodecanoyl phosphatidylcholine (NBD-PC; which is converted to NBD-PA by PLD), treated with 10 μ M ABA, and tracked by lysis and immunoprecipitation with an HA antibody. In the absence of ABA treatment, the amount of NBD-PA precipitated with wild-type RbohD 160 fragments was about threefold greater than that with the quadruple mutant protein fragment. ABA treatment of GCPs for 10 min resulted in a 45% increase in the amount of PA associated with wild-type RbohD160 but not with the mutant (Figure 8B, bottom panel). When Ala and Leu (residues 156 and 157) in RbohF (corresponding to residues 149 and 150 in RbohD) were mutated to Arg and Arg (Figure 8C), the amount of PA associated with RbohF increased greatly in the presence of ABA (Figure 8D). The data confirm the PA-Rboh interaction in guard cells and highlight the importance of residues R(149,150) (RbohD) in PA binding.

PA Binding Stimulates RbohD NADPH Oxidase Activity

To analyze the effect of the PA-Rboh interaction on NADPH oxidase activity, we expressed HA-tagged full-length RbohD in GCPs that were isolated from *rbohD* leaves and measured the resulting ROS production. The RbohD protein expressed in the GCPs was detected by immunoblotting with an HA antibody (Figure 9A). We first measured O_2^- production in GCPs transfected with *RbohD*-HA and empty vector based on the reduction of XTT. Overexpression of RbohD induced significant increases in O_2^- production. Addition of 16:0-18:2 PA further stimulated O_2^- production in the transfected cells. By contrast, 16:0-18:2 PC had no such stimulation on O_2^- generation (Figure 9B). The PA activation of RbohD-mediated ROS generation was tested with the fluorescent dye H_2DCFDA . PA, but not PC, was found to stimulate ROS generation in the GCPs expressing RbohD, whereas PA had a negligible effect on ROS production in GCPs transfected with empty vector (Figure 9C). The results suggest that PA specifically stimulates ROS production in GCPs expressing RbohD.

To directly establish if PA-RbohD binding is important for PA-activated generation of ROS in GCPs, we compared the effect of PA on ROS production in *rbohD* GCPs expressing wild-type RbohD with those expressing the non-PA-binding quadruple mutant. In GCPs expressing the quadruple mutated RbohD protein, PA or PC had no effect on ROS production. However, in GCPs expressing wild-type RbohD, PA, but not PC, increased

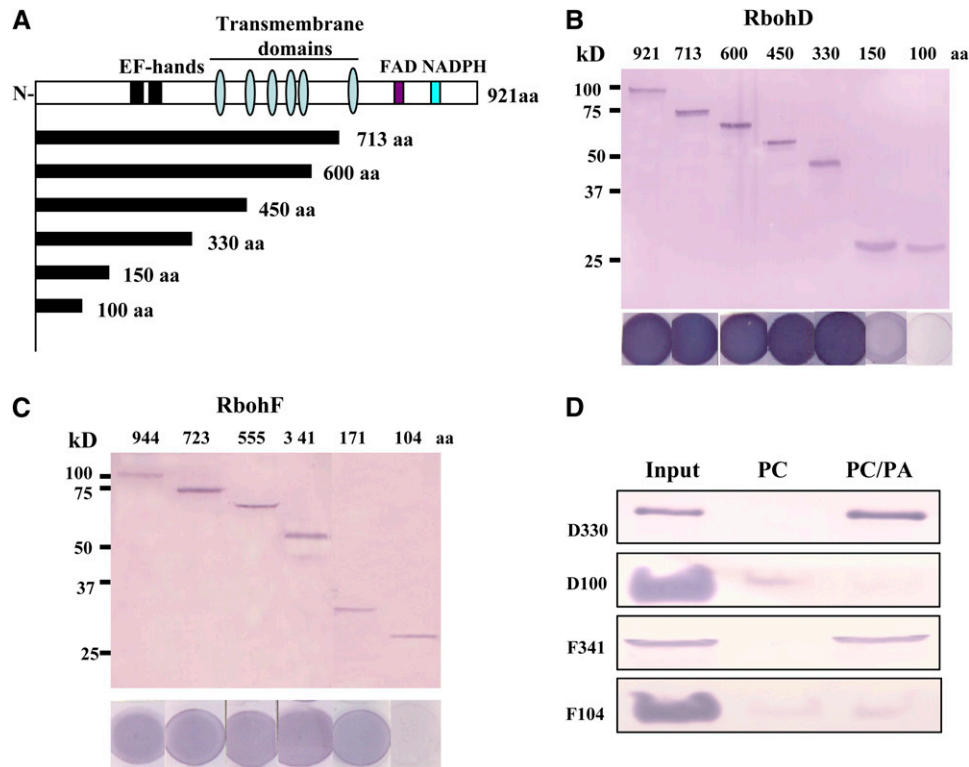


Figure 6. Characterization of the PA Binding Domain of RbohD and RbohF.

(A) Schematic diagram of Rboh protein with the functional domains and deletion structures used in recombinant protein expression and PA binding indicated. Flavin adenine dinucleotide (FAD) and NADPH binding domains, two EF-hands, and six transmembrane domains are shown.

(B) Immunoblotting of His-tagged RbohD N-terminal fragments expressed in *E. coli* (top panel) and 16:0-18:2 PA binding on filters using the same proteins as in the upper panel (bottom panel).

(C) Immunoblotting of His-tagged RbohF N-terminal fragments (top panel) and 16:0-18:2 PA binding on filters using the same proteins as in the upper panel (bottom panel).

(D) RbohD and RbohF fragments bind to liposomes containing 16:0-18:2 PA. 200 μ L of RbohD fragment D330 (D330) and RbohF fragment F341 (F341) (0.5 μ g/ μ L), and 200 μ L of D100/F104 (1.25 μ g/ μ L of each protein) were mixed with 200 μ L of lipid vesicles comprised of 16:0-18:2 PC:PA (3:1) or PC. The vesicles were pelleted by centrifugation, and the liposomal binding proteins were detected by immunoblotting with anti-His antibody. Twenty percent of the proteins used for liposome binding were loaded as a control (input).

[See online article for color version of this figure.]

ROS production significantly (Figure 9D). All of the above data demonstrate that PA-RbohD binding leads to the activation of RbohD NADPH oxidase activity and ROS generation.

The PA-Rboh Interaction Regulates ABA-Mediated ROS Generation and Stomatal Closure

We then asked whether the PA-Rboh interaction is essential for PA- and ABA-mediated ROS generation and stomatal closure. To address this question, we expressed full-length RbohD tagged with green fluorescent protein (GFP) in *rbohD* using an in planta transient transformation assay (Marion et al., 2008). As shown in Figures 10A to 10C, GFP expression was observed in epidermal cells, including guard cells. Wild-type RbohD and non-PA-binding RbohD [quadruple mutation R(149,150,156,157)A] proteins had similar patterns of expression in cotyledons, according to the GFP fluorescent density (Figures 10A to 10C, inset).

As compared with the GFP vector control, overexpression of wild-type RbohD protein resulted in significant stomatal closure in the absence of ABA, whereas overexpression of the non-PA-binding RbohD led to slight stomatal closure (Figure 10D). Cotyledons became yellow in seedlings transiently expressing wild-type RbohD (see Supplemental Figure 8 online). When 2 μ M ABA was applied to the cotyledons, the stomata closed in plants carrying the vector or wild-type RbohD protein. By contrast, ABA-induced stomatal closure was impaired in plants expressing the non-PA-binding RbohD protein (Figure 10D). PA induced stomatal closure in plants expressing wild-type RbohD but not in those carrying the vector or non-PA-binding RbohD. PC had no effects on stomatal closure in any tested plants (Figure 10D). ROS production in the cotyledons of these plants was analyzed by 3,3'-diaminobenzidine staining. The results showed that ABA induced ROS production in guard cells of the cotyledons transformed with wild-type RbohD but that ROS production was

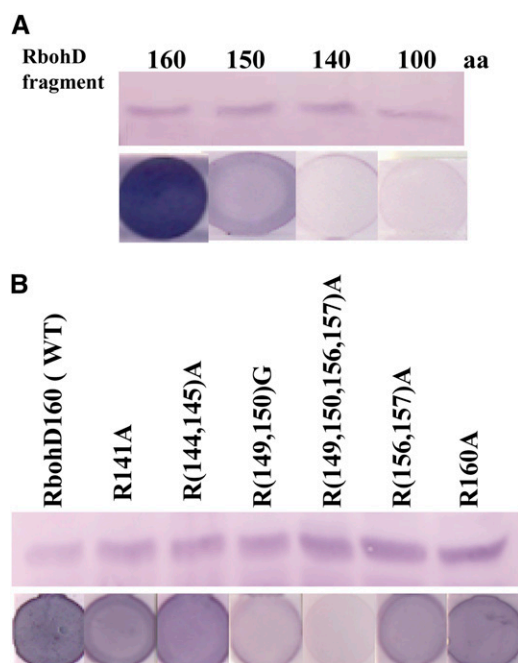


Figure 7. Identification of PA Binding Sites in RbohD.

(A) Binding of RbohD fragments to PA. Top panel: immunoblotting of N-terminal fragments (1 to 100, 140, 150, and 160 amino acids, respectively) expressed in *E. coli*. Bottom panel: binding of protein fragments to PA on filters.

(B) Expression of mutated RbohD fragments and detection of PA binding. Top panel: immunoblotting of wild-type and mutated RbohD160 fragments expressed in *E. coli*. Bottom panel: binding of RbohD160 fragments to PA on filters using the same protein as in the top panel. [See online article for color version of this figure.]

seriously impaired in the guard cells of cotyledons transformed with non-PA-binding RbohD (see Supplemental Figure 9 online). Taken together, these results demonstrate that the PA–RbohD interaction is necessary for ABA-mediated ROS generation and stomatal closure.

We next compared the effects of PA and of ABA on ROS production in guard cells and stomatal closure in *pldα1*, *rbohD*, and *rbohF* mutants. The ABA-induced ROS increase in guard cells was abolished in *pldα1* but was considerably reduced in *rbohD* and *rbohF*. PA increased ROS generation in the wild type and *pldα1* but not in *rbohD* and *rbohF*. PC and LysoPA did not stimulate ROS production in any of the four genotypes (Figure 11A; see Supplemental Figure 10 online).

pldα1 plants were insensitive to ABA promotion of stomatal closure. ABA-induced stomatal closure was partially inhibited in the *rbohF* mutant, but *rbohD* exhibited the same response to ABA-induced stomatal closure as did the wild type (Figure 11B). This result was consistent with that reported by Kwak et al. (2003), who monitored ABA-induced stomatal closure in *RbohD* knockout plants carrying a single *dSpm* transposon insertion. However, wild-type and *pldα1* plants were sensitive to PA-promoted stomatal closure, whereas *rbohD* and *rbohF* were not (Figure 11B). PC had no effect on stomatal closure in any tested

genotype (Figure 11B). By contrast, the application of H_2O_2 induced stomatal closure in the wild type, *pldα1*, *rbohD*, and *rbohF* (Figure 11C). These results indicate that PLD α 1, PA, RbohD, and RbohF all act upstream of ROS.

NO Acts Downstream of PLD α 1, PA, and ROS

In addition to ROS, nitric oxide (NO) is also involved in ABA-induced stomatal closure (Desikan et al., 2002, 2004). ABA-induced ROS production is reported to mediate NO synthesis (Bright et al., 2006). To investigate the role of PLD α 1 and PA in NO production and the relationship between PA, ROS, and NO, we measured NO production in wild-type and *pldα1* guard cells. Treatment with ABA increased NO production in the wild type, but the increase was greatly reduced in *pldα1* guard cells (Figures 12A and 12B). However, application of H_2O_2 increased NO generation in both wild-type and *pldα1* guard cells (Figures 12A and 12B), and the magnitude of increase was similar in these genotypes (Figure 12B). When the NO scavenger 2-phenyl-4,4,5,5-tetramethylimidazolinone-1-oxy 3-oxide (PTIO) was present, the ABA-induced NO increase was greatly reduced. Such decrease in NO production was also found when 1-butanol was used to decrease PA production (Figure 12C). 1-Butanol decreases PLD-mediated formation of PA because PLD can transfer the phosphatidyl group to primary alcohols to produce phosphatidylalcohol at the expense of PA. As a control, 2-butanol, which is not a substrate of PLD, was used and was found not to reduce NO formation (Figure 12C). When a NO donor, sodium nitroprusside (SNP), was used, an increase in NO occurred in both wild-type and *pldα1* guard cells (Figure 9B). 1-Butanol did not affect SNP-produced NO increase (Figure 12C). As with H_2O_2 , NO (SNP) induced stomatal closure in both wild-type and *pldα1* plants (Figure 12D). These data indicate that PLD α 1 and PA are involved in promoting ABA-induced NO production and that NO functions downstream of ROS.

The PA and ABI1 Interaction Is Important for ROS and NO Signal Transduction

Previous studies showed that one mechanism by which PLD α 1 mediates ABA-promoted stomatal closure is through PA binding to ABI1 to inhibit its function (Zhang et al., 2004). This raises intriguing questions as to whether PA and ABI1 interaction is essential for the production of ROS and NO and/or their signal transduction in guard cells. To address these questions, we compared ROS production in guard cells of wild-type plants and in those of the non-PA-binding mutant (*ABI1_{R73A}*). This mutant was generated by expressing *ABI1_{R73A}*, driven by the ABI1 native promoter, in an *ABI1*-knockout (*abi1*) background (Mishra et al., 2006). *ABI1_{R73A}* has normal phosphatase activity but cannot bind to PA (Zhang et al., 2004). The *ABI1_{R73A}* transgenic plants exhibited the ABA-induced increases in ROS levels similar to wild-type cells (Figure 13A). Likewise, ABA-induced NO generation was also similar in wild-type and *ABI1_{R73A}* plants (Figure 13B).

However, *ABI1_{R73A}* plants were insensitive to the promotion of stomatal closure by ABA, ROS, or NO, whereas wild-type plants were sensitive (Figure 13C). These data indicate that the PA–ABI1 interaction is not required for ROS or NO production but

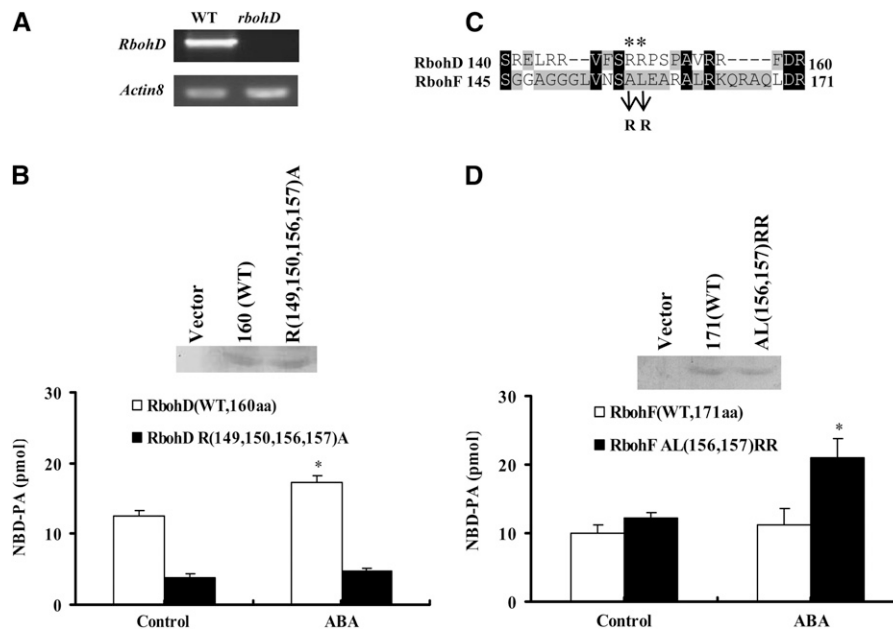


Figure 8. Quantification of Fluorescent PA Bound to RbohD and RbohF Fragments Expressed in GCPs.

(A) RT-PCR analysis of *RbohD* gene expression in the wild type and *rbohD* mutant. The experiment was repeated three times under the same conditions.

(B) Quantification of fluorescent PA bound to wild-type and non-PA-binding RbohD fragments. Top panel: immunoblotting of HA-tagged RbohD fragments (160 amino acids) of the wild type and non-PA-binding mutant [R(149,150,156,157)A] expressed in *rbohD* GCPs. Bottom panel: quantification of fluorescent NBD-PA coimmunoprecipitated with RbohD fragments in the absence or presence of 10 μ M ABA for 10 min.

(C) Amino acid alignment of the PA binding region in RbohD and corresponding region in RbohF. The double mutation [AL(156,157)RR] in the RbohF sequence is indicated.

(D) Quantification of fluorescent PA bound to wild-type and double mutant RbohF [AL(156,157)RR] fragments. Top panel: immunoblotting of RbohF fragments of the wild type and double mutant [AL(156,157)RR]. Bottom panel: quantification of fluorescent NBD-PA coimmunoprecipitated with RbohF fragments in the absence or presence of 10 μ M ABA for 10 min.

Data in **(B)** and **(D)** are means \pm SE of three independent experiments.

that the PA-ABI1 interaction is involved in mediating the effect of ROS and NO on stomatal closure. The *abi1* plants produced similar amounts of ROS and NO in response to ABA treatment as the wild-type plants and had similar degrees of stomatal closure following ABA, H₂O₂, or NO treatment as the wild type (Figure 13). These similarities are consistent with the notion that ABI1 is a negative effector in the ABA response.

DISCUSSION

Recent work in nerve cells has revealed functions for lipids in protein trafficking, cellular communication, and the production of the hundreds of molecules that carry information both within and across cells (Piomelli et al., 2007). Lipids can regulate ion channels, receptors, and other signal transduction proteins, not only by influencing the curvature or supramolecular organization of the membrane, but also by directly binding to the proteins (Hancock, 2007; Piomelli et al., 2007). There is no doubt that lipids can act as signal messengers in plant cells (Wang et al., 2006; Munnik and Testerink, 2009; and references within). Plant PLD and derived PA are involved in ABA-mediated stomatal movement by interaction with the α -subunit of G protein,

through PA regulation of the inwardly rectifying K⁺ channel, and/or ABI1 PP2C localization and activity (Jacob et al., 1999; Zhang et al., 2004; Mishra et al., 2006). Other lipids, including phosphoinositides and sphingolipids, are also important regulators of ABA-mediated stomatal movement (Jacob et al., 1999; Coursol et al., 2003; Park et al., 2003; Perera et al., 2008). However, much less is known about lipid functions in cell signaling and their mechanisms in plant cells than in animal cells. In this study, we have identified the transmembrane protein Rboh as a direct target of the lipid messenger PA, which is derived from ABA-activated PLD α 1 and showed that PA-RbohD interaction is essential to ABA-mediated ROS production and stomatal closure.

Rbohs Are Intermediates of PLD Signaling in ABA-Mediated Stomatal Closure

Both PLDs and NADPH oxidases play important roles in producing signals that mediate the cellular response to environmental stress by activation of downstream targets (Bargmann and Munnik, 2005; Torres and Dangl, 2005; Wang, 2005; and references within). We showed here that PLD α 1 and PA were required for the production of ROS in guard cells in response to ABA and that PA directly interacts with Rboh. The conclusion is

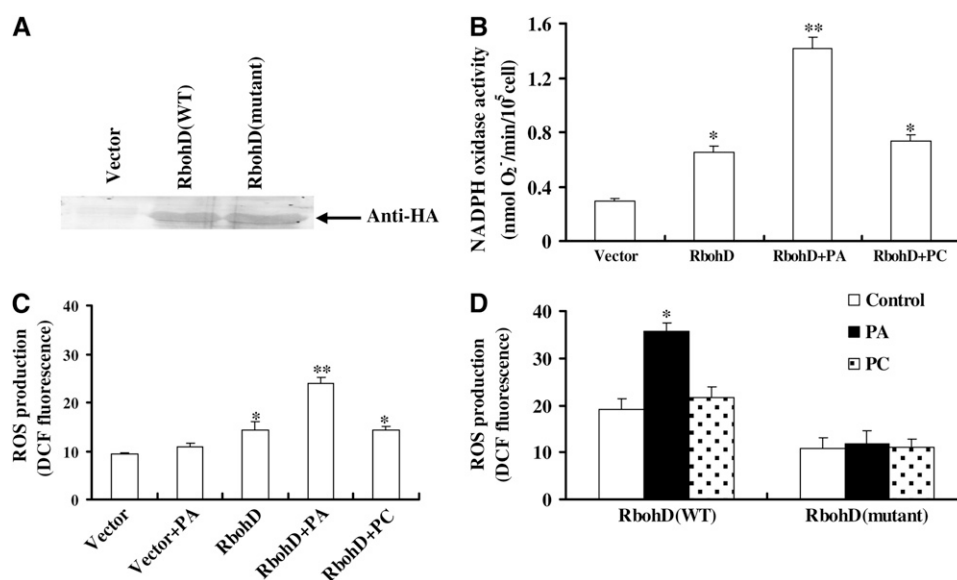


Figure 9. PA Stimulates RbohD Activity.

(A) Immunoblotting of full-length proteins of the wild type and the non-PA-binding mutant RbohD expressed in *rbohD* GCPs. The proteins were separated by SDS-PAGE and probed with anti-HA antibody. The empty vector with HA tag was used as a control.

(B) The effect of PA on RbohD activity. RbohD-HA or empty vector was expressed in *rbohD* mutant GCPs for 4 h. Reaction buffer and 1 μ M 16:0-18:2 PA (or 16:0-18:2 PC) were added to GCPs for 10 min. After centrifugation, the supernatant was used for spectrophotometric analysis of XTT formazan production at A_{470} . NADPH activity calculation is described in Methods. Data are means \pm SE of 4×10^4 GCPs per treatment per experiment.

(C) The effect of PA on ROS production in GCPs expressing RbohD. RbohD-HA or empty vector was expressed in *rbohD* mutant GCPs for 4 h. A total of 1 μ M 16:0-18:2 PA (or 16:0-18:2 PC) was added to the GCPs for 10 min after the GCPs were stained with H₂DCFDA for 10 min. Confocal images were quantified as mean pixel intensities \pm SE; $n = 60$ cells per treatment per experiment.

(D) The effect of PA on ROS production by wild-type and mutated RbohD. RbohD-HA or RbohD-HA with R(149,150,156,157)A mutations was expressed in *rbohD* GCPs for 4 h, followed by DCF fluorescence assaying of ROS production. Confocal images were quantified as mean pixel intensities \pm SE; $n = 55$ cells per treatment per experiment.

Data in **(B)** to **(D)** are means \pm SE of three independent experiments. The asterisk in **(B)** and **(C)** indicates that the mean value is significantly different from that of the vector (one asterisk for $P < 0.05$; two asterisks for $P < 0.01$). An asterisk in **(D)** indicates that the mean value is significantly different from the control ($P < 0.05$).

supported by several lines of evidence. (1) ABA-induced ROS production was impaired in *pld α 1* guard cells. When H₂O₂ was added, stomata closed in *pld α 1*, as well as in wild-type plants. (2) The ABA-stimulated increase in NADPH oxidase activity was reduced in *pld α 1* GCPs, whereas addition of PA restored NADPH oxidase activity. The data suggest that PLD α 1-derived PA is an activator of NADPH oxidase. (3) PA species 34:1(16:0-18:1), 34:2(16:0-18:2), and 36:3(18:1-18:2) were significantly increased 10 min after ABA application, producing potential PA sources for binding to the NADPH oxidases (RbohD and RbohF) because PA species with 18:1 or 18:2 fatty acids were bound to the Rbohs. (4) 16:0-18:2 PA, one of the PA species increased most by ABA, was found to bind to RbohD and RbohF in vitro and in vivo. (5) The disruption of PA-Rboh (RbohD) binding compromised ABA-mediated ROS production and stomatal closure.

The 34:2 (16:0-18:2) PA and other PA species were also increased in the *pld α 1* mutant treated with ABA, although the magnitude and absolute amount of the increase was lower than in the wild type. The results suggest that there are other enzymes that respond to ABA to produce PA. In *Arabidopsis*, multiple PLDs have diverse functions in response to environmental and

developmental stimuli (Wang, 2005), and some of them are probably activated by ABA treatment. In addition, DGK may phosphorylate diacylglycerol that is produced from PLC, which is known to be activated by ABA; the coupled PLC/DGK is another route that produces signaling PA (Testerink and Munnik, 2005; Wang et al., 2006). DGKs play a role in plant development (Gómez-Merino et al., 2005), but whether they are involved in the ABA response remains to be investigated.

The difference in magnitude in ABA-induced PA increase between the wild type and *pld α 1* mutant is probably one of reasons for lower NADPH oxidase activity and ROS generation in response to ABA in the mutant guard cells, as the amount of PA-bound Rbohs increased with increasing PA concentrations (see Supplemental Figure 11 online). PA binding to NADPH oxidase is essential for Rboh(D) activation. Even in the control condition, NADPH oxidase activity in the *pld α 1* mutant was lower than in the wild type, which may contribute to the greater water loss from mutant plants during the 3-d growth period (see Supplemental Figure 12 online). This is consistent with results obtained from PLD α -antisense suppressed plants that had an earlier drought phenotype after withholding irrigation than did the wild type. In

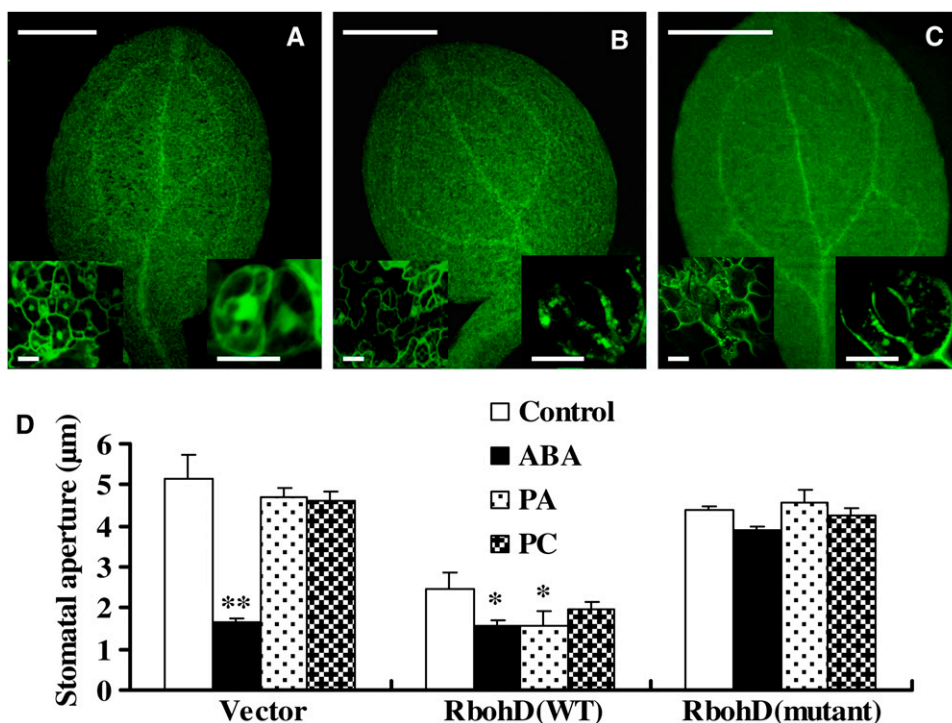


Figure 10. Abrogation of PA-RbohD Binding Impairs ABA-Induced Stomatal Closure.

(A) to (C) Transient expression of wild-type and non-PA-binding RbohD fused to GFP in *rbohD* seedlings. RbohD-GFP was visualized in whole cotyledons, in epidermal cells (left bottom), and in guard cells (right bottom). Cotyledons transformed with GFP alone (A), RbohD-GFP (B), and non-PA-binding RbohD-GFP (C). Bars = 0.5 mm for cotyledons and 10 μ m for insets.

(D) Changes in stomatal aperture in response to ABA, PA, and PC. *rbohD* seedlings expressing GFP vector, RbohD-GFP, or non-PA-binding RbohD-GFP were incubated with 2 μ M ABA or 50 μ M 16:0-18:2 PA (or 16:0-18:2 PC) for 2 h, and stomatal apertures were measured. Data are means \pm SE of three independent experiments; $n = 65$ apertures per treatment per experiment. The asterisk indicates that the mean value is significantly different from that of the control (one asterisk for $P < 0.05$; two asterisks for $P < 0.01$).

addition, applied ABA could not alleviate the drought phenotype in the mutant, but it enhanced the tolerance to drought in the wild-type plants (Sang et al., 2001b).

Although it showed a lower level of NADPH oxidase activity and ROS generation than the wild type, *pld α 1* had a background level of ROS before ABA treatment. Besides NADPH oxidase, there are intracellular and extracellular routes for ROS production in plants. Inside the plant cell, ROS can be produced as byproducts of photosynthesis and respiration. In the apoplast, ROS can be generated by cell wall-bound peroxidases, oxalate oxidases, and amino oxidases (Torres and Dangl, 2005; An et al., 2008). These pathways together with ROS scavengers may contribute to basal ROS homeostasis. Despite this, our data from the plasma membrane, guard cells, and plants show that PLD α 1 and PA are important regulators of plasma membrane-associated NADPH oxidase activity in response to ABA in stomatal closure.

PA-Rbohs Interaction Suggests a Novel Regulatory Mechanism for Plant NADPH Oxidase

In mammalian systems, PA activates NADPH oxidase via interaction with the regulatory subunit p47^{phox}. The mammalian

NADPH oxidase component p47^{phox} has a PX domain with two distinct lipid binding sites. Simultaneous occupancy of the PA and PtdInsP₂ binding sites leads to a synergistic increase in membrane affinity of the protein (Karathanassis et al., 2002). However, the *Arabidopsis* genome has no ortholog of p47^{phox}, and Rboh proteins do not contain a PX or PH domain (Torres and Dangl, 2005). The PA binding region of RbohD shares little sequence similarity with that of p47^{phox} (Karathanassis et al., 2002) but more sequence similarity with the ABI1 PA binding motif in plants (Zhang et al., 2004; 20% versus 30%). The amino acid sequence of the PA binding region (140 to 160 amino acids for RbohD and 145 to 171 amino acids for RbohF) is not highly conserved between RbohD and RbohF (Figure 8C). The major PA binding basic residues (Arg-149 and -150) in RbohD are replaced with nonpolar residues Ala-156 and Leu-157 in RbohF. Simultaneous mutation of Ala-156 and Leu-157 to Arg in RbohF resulted in an increase in PA binding after ABA treatment. The results indicate that the difference between the two major PA binding residues of RbohF (Ala-156 and Leu-157) and RbohD (Arg-149 and Arg-150) may contribute to lower PA binding in RbohF. We do not rule out the possibility that other mediators of RbohF regulation, such as Rac (Wong et al., 2007), Ca²⁺ (Ogasawara et al.,

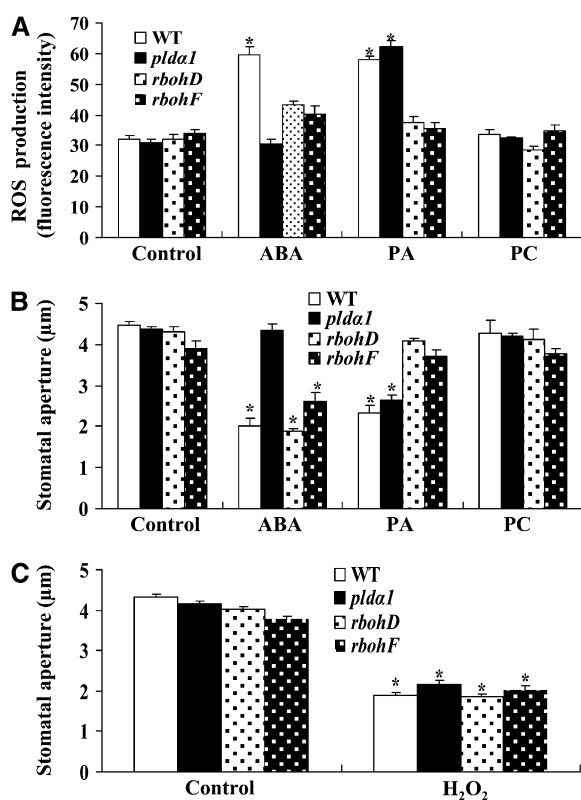


Figure 11. Abrogation of RbohD and RbohF Alters ABA- and PA-Induced ROS Production and Stomatal Closure.

(A) ROS production in guard cells in response to ABA or lipids. Epidermal peels preloaded with H₂DCFDA for 10 min were treated with 50 μ M ABA for 5 min or 50 μ M 16:0-18:2 PA (or 16:0-18:2 PC) for 8 min. Confocal images were quantified as mean pixel intensities. Values are means \pm SE; $n = 50$ per genotype per experiment.

(B) Changes in stomatal aperture after ABA or lipid treatment. Stomatal apertures were measured after 2.5 h of treatment. Values are means \pm SE; $n = 65$ apertures each genotype per experiment.

(C) Addition of H₂O₂ induces stomatal closure. Stomatal apertures were measured after 2 h of treatment with H₂O₂. Values are means \pm SE; $n = 80$ apertures per genotype per experiment.

Data in **(A)** to **(C)** are from three independent experiments. The asterisk in **(A)** to **(C)** indicates that the mean value is significantly different from that of the corresponding control ($P < 0.05$).

2008), and CDPK (Kobayashi et al., 2007), have a role in the ABA response.

Knockout of *RbohF* results in less sensitivity to ABA-induced stomatal closure than the wild type and *rbohD* (Kwak et al., 2003; Figure 11). It seems that RbohF plays a more important role than RbohD in ABA-mediated stomatal closure. The *rbohD/F* double mutant was more impaired in ABA-induced stomatal closure than *rbohF* or the *rbohD/E* double mutant (Kwak et al., 2003). Conversely, overexpression of wild-type *RbohD* led to stomatal closure (Figure 10D) as well as ROS increase even in the absence of ABA (Figure 9C; see Supplemental Figure 9 online). The results suggest that both RbohD and RbohF are major enzymes in ROS generation during ABA response. These proteins probably have

overlapping functions or interactions during ABA-induced ROS generation in guard cells and in the pathogen response (Kwak et al., 2003; Torres and Dangl, 2005). Furthermore, the overexpression of the non-PA-binding Rboh protein in *rbohD* mutant impaired ABA-induced stomatal closure. It seems that the introduction of the non-PA-binding protein has a dominant-negative effect, which could result from the interference of the overexpressed protein with other Rbohs and/or with cellular effectors of Rbohs.

Knockout of *RbohD* and *RbohF* both impaired the increase of ROS production in guard cells exposed to ABA. PA could not induce ROS production in guard cells of these mutants. Therefore, the PA-Rboh interaction is essential to ABA-mediated ROS production, regardless of RbohD or RbohF, although their PA binding abilities are different. Using a transient expression system, we have demonstrated directly the importance of PA-RbohD binding in ABA-induced stomatal closure in planta. However, an interesting question still remains as to why ROS generation in both *rbohD* and *rbohF* is impaired, but ABA-induced stomatal closure is more impaired in *rbohF* than in *atrbohD*. In fact, when expression of the ABA-responsive gene *RAB18* was assayed in these mutants, we found that *RAB18* expression was enhanced in *rbohD* but was abolished in *atrbohF* (see Supplemental Figure 13 online). These results suggest that RbohD and RbohF have different functions in mediating the ABA response.

The mechanism by which PA regulates the NADPH oxidases is different from that of other lipids, such as PtdIns(3)P, which participates in ABA-induced ROS generation and stomatal closure (Park et al., 2003). PtdIns(3)P is synthesized by phosphatidylinositol 3-kinase. Both PtdIns(3)P and phosphatidylinositol 3-kinase are involved in ROS production in root hairs (Lee et al., 2008) or roots exposed to salt stress treatment (Leshem et al., 2007). In this work, we did not detect binding of PtdIns(3)P or PtdIns(4)P to RbohD or RbohF (see Supplemental Figure 5 online). In root systems, phosphatidylinositol signaling is thought to regulate the intracellular assembly of the active NADPH oxidase complex by endocytotic membrane trafficking (Leshem et al., 2007); PA binding may not be involved in this pathway.

The PA binding site in RbohD was located in the cytosolic region between the two EF-hands and N terminus (Figure 14). Recently, Kobayashi et al. (2007) reported CDPK-mediated phosphorylation of StrbohB at Ser-82 and Ser-97 in potato. RbohD and StrbohB have a high degree of amino acid identity, and both have the conserved phosphorylation motif B-X-X-S (where B is a basic residue, S is a Ser residue, and X is any residue). It is worth noting that the major PA binding residues (Arg-149 and -150) are in the vicinity of the B-X-X-S motif (Kobayashi et al., 2007; see Supplemental Figure 4 online). Phosphorylation was proposed to induce conformational changes in RbohB, leading to the interaction with the small GTPase Rac in the vicinity of the EF-hand motifs (Wong et al., 2007). However, the phosphorylation of Rboh is not sufficient for full activation of Rboh (Kobayashi et al., 2007; Nuhse et al., 2007), implying that there may be additional determinants that can regulate the activity. As discussed above, the binding of Rbohs by the lipid messenger PA identified in this study may reveal a novel regulatory mechanism for Rboh activation. As PA

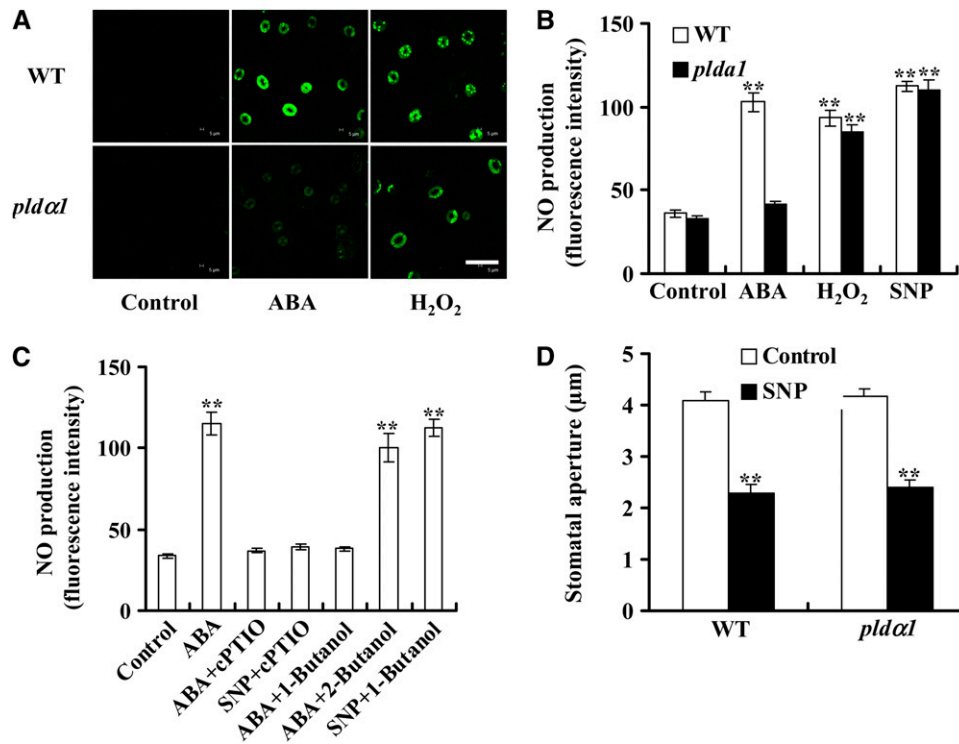


Figure 12. PLD α 1 and PA Mediate ABA-Induced NO Production.

(A) Representative images of NO production indicated by the fluorescent dye DAF-2DA. Epidermal peels were loaded with 10 μ M DAF-2DA for 10 min before the addition of ABA (50 μ M) or H₂O₂ (100 μ M) for another 10 min. Bar = 50 μ m.

(B) NO production in guard cells induced by ABA and H₂O₂. The NO donor, SNP (100 μ M), was used as a positive control for NO production. Data are means \pm SE; n = 70 per genotype per experiment.

(C) Inhibition of ABA-induced NO production by 1-butanol. Epidermal peels were preincubated with 200 μ M PTIO for 30 min before ABA (50 μ M) or SNP (100 μ M) treatment; 0.1% (v/v) 1- or 2-butanol was added together with ABA, and 1-butanol was added together with SNP. Data are means \pm SE; n = 65 per treatment per experiment.

(D) NO induced stomatal closure in wild-type and *pldα1* plants. The epidermal peels were treated with 100 μ M SNP. Data are means \pm SE; n = 80 per genotype per experiment.

Data in **(B)** to **(D)** are from three independent experiments. Two asterisks indicate that the value is significantly different from that of the control ($P < 0.01$).

production is induced by a wide spectrum of stimuli (Wang et al., 2006), this mechanism is likely to have a central role in the coupling of extracellular signals to Rboh activation.

A Complex Signaling Network Involving PA, ROS, NO, and ABI1 in ABA-Mediated Signaling during Stomatal Closure

Several targets downstream of ROS have been reported to respond to ABA treatment in guard cells. These include protein kinases, protein phosphatases, ion channels, and NO (Li et al., 2006; Neill et al., 2008; and references within). Pharmacological and genetic evidence reveals that NO accumulation induced by ABA in guard cells is dependent on ROS (Bright et al., 2006). NO selectively regulates K⁺ and Cl⁻ channels in *Vicia faba* guard cells by enhancing cytosolic Ca²⁺ release from intracellular Ca²⁺ stores, which leads to solute loss and stomatal closure (Garcia-Mata et al., 2003). Using the dominant-negative *abi1-1* and *abi2-1* mutants, ABI1 and ABI2 protein phosphatases have been placed

downstream of NO in the ABA signal transduction cascade in guard cells (Desikan et al., 2002). We previously showed that PA interacts directly with ABI1, which leads to membrane tethering of ABI1 and a decrease in its PP2C activity (Zhang et al., 2004). ABI1 is a negative regulator of ABA action. The recruitment of ABI1 to the plasma membrane and the inhibition of its activity are essential for preventing its interaction with the transcription factor ATHB6 and, therefore, for transducing the ABA signal (Zhang et al., 2004; Mishra et al., 2006). This could explain why the disruption of PA-ABI1 did not affect ABA-induced ROS and NO production but inhibited H₂O₂- and NO-induced stomatal closure. These results suggest that PA-ABI1 interaction is downstream of ROS and NO signaling and that the interaction is necessary for both ROS- and NO-mediated stomatal closure.

ROS and NO may also act independently in ABA-evoked stomatal closure. For example, H₂O₂ elevates the concentration of Ca²⁺ in the cytosol by regulating Ca²⁺ gating in the plasma

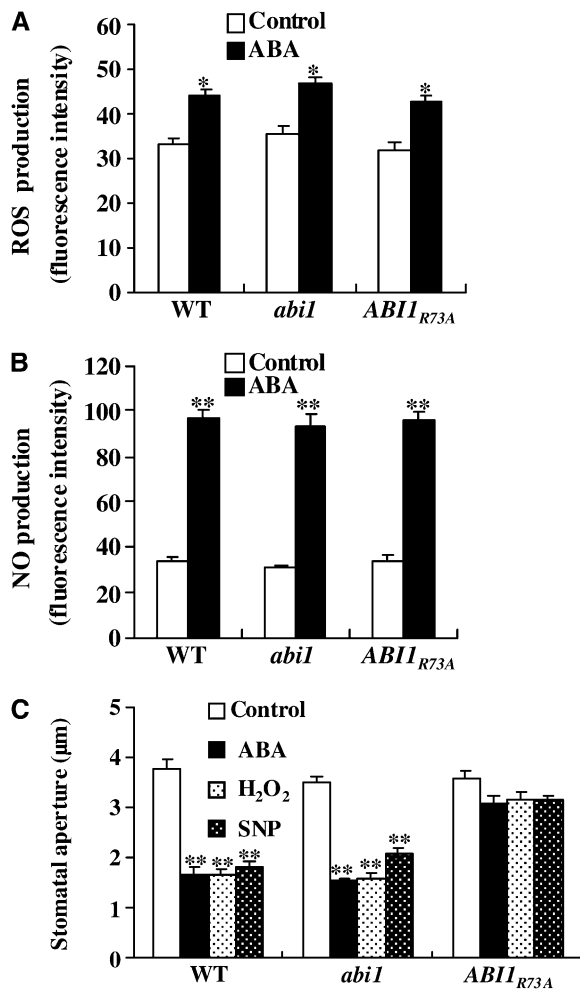


Figure 13. Disruption of PA-ABI1 Binding Affects ROS or NO Promotion of Stomatal Closure but Not ROS or NO Production.

(A) ROS production in guard cells as monitored by H₂DCFDA. The epidermal peels were treated with 50 µM ABA for 5 min. Data are means ± SE; *n* = 60 per genotype per experiment.

(B) NO production in guard cells as monitored by DAF-2DA. The epidermal peels were treated with 50 µM ABA for 10 min. Data are means ± SE; *n* = 65 per genotype per experiment.

(C) Changes in stomatal aperture in response to ABA, H₂O₂, and NO. The epidermal peels with fully opened stomata were incubated with 50 µM ABA, 100 µM H₂O₂, or 100 µM SNP. Stomatal apertures were measured after 2.5 h of treatment. Data are means ± SE; *n* = 80 apertures per genotype per experiment.

Values in **(A)** to **(C)** are means ± SE of three experiments. The asterisk indicates that the mean value is significantly different from that of the corresponding control (one asterisk for *P* < 0.05; two asterisks for *P* < 0.01).

membrane in guard cells (Pei et al., 2000), instead of drawing on the intracellular Ca²⁺ store via NO (Garcia-Mata et al., 2003). A very low level of NO has no influence on outward-rectifying K⁺ channels, while a moderate elevation of NO results in a decrease in K⁺ channel activity, which is reversed by a reducing reagent

(Garcia-Mata et al., 2003; Sokolovski and Blatt, 2004). H₂O₂ suppresses both inward- and outward-rectifying K⁺ channels (Köhler et al., 2003), but the residual activity of outward-rectifying K⁺ channels may be sufficient for K⁺ efflux after H₂O₂ application (Kwak et al., 2006, and references within). Therefore, it is reasonable to hypothesize that ROS and NO may function harmoniously and/or in parallel to regulate K⁺ channels in the ABA response.

In vitro analyses indicate that H₂O₂ could in turn inactivate the enzymatic activities of ABI1 and ABI2 PP2Cs (Meinhard and Grill, 2001; Merlot et al., 2001; Meinhard et al., 2002). ROS produced by PA-Rboh interaction may inhibit ABI1 activity, which is likely another mechanism by which PA regulates stomatal closure. On the other hand, recent evidence shows that NO triggers PA accumulation during auxin-induced adventitious root formation (Lanteri et al., 2008) and elicitor response (Laxalt et al., 2007). Whether such a feedback regulation loop exists in ABA-mediated stomatal closure needs to be tested.

In conclusion, this study demonstrates a novel role for PLD/PA-mediated ABA signaling pathway in stomatal closure and for the Rboh regulation in plants. Activation of PLD by ABA results in PA production. PA binds to the cytosolic region in the N-terminus of Rboh(D), resulting in the stimulation of NADPH oxidase activity and ROS production in guard cells. PA-Rboh interaction is essential for ABA-mediated ROS production and stomatal closure. Other regulators, such as Rac, Ca²⁺, CDPKs, and MAPK cascades are probably involved in the processes. ROS regulates channel activity through NO or independently, leading to solute loss and stomatal closure. On the other hand, the PA-ABI1

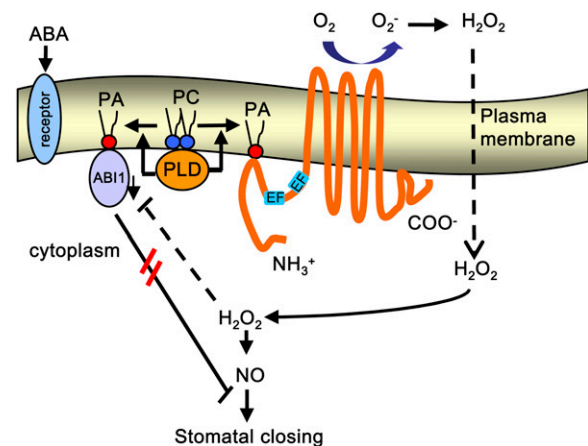


Figure 14. Working Model of PA Activation of Rboh in ABA-Induced Stomatal Closure in *Arabidopsis*.

ABA stimulates PLD activity probably through a putative ABA receptor. The lipid messenger PA produced by ABA activation of PLD binds to Rboh in the cytosolic region of the N terminus. The activation of Rboh by PA binding results in ROS production (including H₂O₂). The PA-ABI1 interaction impairs ABI1 inhibition of H₂O₂ and NO signaling. Possible interactions between the identified components and other intermediates are discussed in the Discussion. The double red lines between ABI1 and stomatal closing indicate that the recruitment of ABI1 to the plasma membrane impairs ABI1 inhibition of stomatal closing.

interaction results in membrane recruitment of ABI1 and a decrease in PP2C activity, thereby antagonizing ABI1's inhibition of H₂O₂ and NO signaling (Figure 14). The interactions of PLD and PA with different effector proteins suggest that the lipid messengers play an important role in the regulation of membrane-associated signaling complexes in plant response to ABA and stresses.

METHODS

Plant Materials and Growth Conditions

Arabidopsis thaliana wild-type and mutant plants were from the Columbia ecotype. Seeds were germinated in soil and kept at 4°C for 2 d. Plants were grown in a growth room at a light intensity of 160 μmol m⁻² s⁻¹ and 12-h/12-h (23°C/18°C) day/night regimes. Four- to six-week-old plants were used to prepare protoplasts and epidermal peels.

Chemicals

Most chemicals were from Sigma-Aldrich. PtdIns were purchased from Echelon Biociences, and other lipids were purchased from Avanti Polar Lipids.

Genotyping of Mutants

The identification and verification of T-DNA-insertion mutants of *PLDα1* (*pldα1*), *ABI1* (*abi1*), and *abi1* complemented with *ABI1*_{WT} (*ABI1*_{WT}) or *ABI1*_{R73A} (*ABI1*_{R73A}) were reported previously (Zhang et al., 2004; Mishra et al., 2006). The T-DNA insertion *RbohD* mutant (*rbohD*, SALK_120299) was obtained from ABRC at Ohio State University (www.arabidopsis.org/abrc). To identify homozygous lines and to confirm the exact insertion position of the T-DNA in the *rbohD* mutant, a PCR-based approach was used. Primers were designed using the SALK T-DNA verification primer design program (signal.SALK.edu/tdnaprimers): *RbohD*-SALK-F/*RbohD*-SALK-R and *LB3.1/RbohD*-SALK-R. Actin 8 was used as an internal control, with primers *Actin8*-F/*Actin8*-R (see Supplemental Table 1 for all primer sequences used in this article). *rbohD* and *rbohF* mutants containing *dSpm* transposon insertions were generous gifts from J.L. Dangel and J.M. Kwak.

RbohD and *RbohF* Cloning and Construction of Expression Vectors

The cDNA sequences of *Arabidopsis* *Rboh* genes *RbohD* and *RbohF* were amplified from leaf cDNA using the following primer combinations: *RbohD*-C-F/*RbohD*-C-R for *RbohD* and *RbohF*-C-F/*RbohF*-C-R for *RbohF*. cDNA fragments for nine C-terminal deletion mutants of *RbohD* were amplified by PCR using *RbohD* cDNA as a template. A common forward primer, *RbohD921F*, was paired with the following nine reverse primers: *RbohD921R* for the full-length *RbohD921* (1 to 921 amino acids), *RbohD713R* for *RbohD713* (1 to 713 amino acids), *RbohD600R* for *RbohD600* (1 to 600 amino acids), *RbohD450R* for *RbohD450* (1 to 450 amino acids), *RbohD330R* for *RbohD330* (1 to 330 amino acids), *RbohD160R* for *RbohD160* (1 to 160 amino acids), *RbohD150R* for *RbohD150* (1 to 150 amino acids), *RbohD140R* for *RbohD140* (1 to 140 amino acids), and *RbohD100R* for *RbohD100* (1 to 100 amino acids). All of these fragments were cloned into a pET28a vector.

cDNAs for the full-length and five C-terminal deletion mutants of *RbohF* were amplified by PCR using *RbohF* cDNA as a template. The same forward primer, *RbohF944F*, was paired with the following reverse primers: *RbohF944R* for *RhohF944* (1 to 944 amino acids), *RbohF723R* for *RhohF723* (1 to 723 amino acids), *RhohF555R* for *RhohF555* (1 to 555

amino acids), *RhohF341R* for *RhohF341* (1 to 341 amino acids), *RhohF171R* for *RhohF171* (1 to 171 amino acids), and *RhohF104R* for *RhohF104* (1 to 104 amino acids). All these fragments were cloned into a pET28a vector.

For PA binding site characterization in *RbohD* and *RbohF*, the Quick-change site-directed mutagenesis kit (Stratagene) was used to generate the site-directed mutants. Using *RbohD160* cDNA as template, the primers used to produce the single mutant R141A and R160A were *R141A-F* and *R141A-R*, and *R160A-F* and *R160A-R*, respectively. The primers used to generate the double mutants R(144,145)A, R(149,150)G, and R(156,157)A were *R(144,145)A-F* and *R(144,145)A-R*, *R(149,150)G-F* and *R(149,150)G-R*, and *R(156,157)A-F* and *R(156,157)A-R*, respectively. The primers for the quadruple mutant R(149,150,156,157)A were *R(149,150,156,157)A-F* and *R(149,150,156,157)A-R*.

For protein expression in *Escherichia coli*, *RbohD* and *RbohF* cDNAs were cloned into a pET28a vector (Novagen) at *EcoRI/NotI* and *BamHI/XhoI* sites, respectively. Fusion proteins were expressed in *E. coli* strain BL21 (DE3; Promega) according to the manufacturer's instructions.

For hemagglutinin (HA)-tagged protein expression in guard cell protoplasts, site-specific mutants were generated using the Quickchange site-directed mutagenesis kit. The cDNAs for native and quadruple mutated HA-*RbohD160* were amplified by PCR using cDNAs of the *RbohD160* and *RbohD160* mutant with R(149,150,156,157)A mutation as templates, respectively. A common forward primer *D-160-HA-F* was paired with the reverse primer *D-160-HA-R* (for native HA-*RbohD160*) and *D-R(149,150,156,157)A-HA-R* (for mutated HA-*RbohD160*). cDNA for the C-terminal deletion HA-*RbohF171* was amplified using *RbohF* cDNA as the template with the *RbohF171-HA-F* and *RbohF171-HA-R* primers. The cDNA for HA-*RbohF171* (AL156-157RR) was generated using native *HA-RbohF171* cDNA as the template with forward primer *F171-AL(156,157)RR-F* and reverse primer *F-AL(156,157)RR-R*. cDNA for full-length native HA-*RbohD* was amplified using *RbohD* cDNA as the template with the *D-160-HA-F* and *D-921-HA-R* primer pair. cDNA for full-length HA-*RbohD* with the quadruple mutation was generated using native *HA-RbohD* cDNA as the template with forward primer *R(149,150,156,157)A-F* and reverse primer *R(149,150,156,157)A-R*.

For the *RbohD* activity assay in protoplasts, *RbohD* cDNA was placed under the control of the 35S promoter and a HA tag was fused to the C terminus (Zhang et al., 2004).

The full-length native *RbohD-GFP* and *RbohD-GFP* with the quadruple mutation were amplified using cDNAs of *RbohD* and *HA-RbohD* with quadruple mutation as the template with gene-specific primers *D-GFP-F* and *D-GFP-R*.

All amplified target sequences were confirmed by DNA sequencing.

RNA Isolation and RT-PCR

Total RNA was extracted from expanded leaves of 5-week-old *Arabidopsis* plants using Trizol reagent (Invitrogen) according to the procedure described by the manufacturer. cDNA was synthesized from 1 μg of total RNA using an oligo(dT) primer and AMV reverse transcriptase (Promega). The *RbohD* transcript was amplified using the gene-specific primers *RbohD-RT-F* and *RbohD-RT-R*. PCR conditions were as follows: 94°C for 4 min; 30 cycles of 94°C for 30 s, 56°C for 45 s, and 72°C for 3 min; and a final extension at 72°C for 10 min. Amplicons were visualized on a 1% agarose gel under UV light. The agarose gel was stained with ethidium bromide.

Expression and Purification of *RbohD* and *RbohF* Proteins in *E. coli*

Recombinant plasmids carrying *RbohD* and *RbohF* with six histidine residues were transformed into *E. coli* BL21(DE3). The proteins were expressed at 25°C for 4 to 5 h. Bacterial cells were harvested and resuspended in lysis buffer (25 mM HEPES, 300 mM NaCl, 0.5% Triton

X-100, 10 mM imidazole, and 1 mM PMSF, pH 8.0). After incubation on ice for 30 min, samples were sonicated and centrifuged at 10,000g for 20 min. The resulting supernatant was used for protein purification with Ni-affinity agarose (Qiagen) according to the manufacturer's instructions.

Purified proteins were used for immunoblotting and the analysis of protein-lipid interaction. For immunoblotting, proteins were separated on an 8% SDS-PAGE gel and immunoblotted with anti-His antibody (Sigma-Aldrich), followed by the secondary antibody conjugated with alkaline phosphatase. Proteins were quantified with the Bradford method using the reagent from Bio-Rad.

Analysis of Protein-Lipid Binding

Protein-lipid interaction was assayed using filter, liposome binding, and ELISA approaches. The filter binding was performed as described (Zhang et al., 2004). Briefly, lipids were immobilized on a nitrocellulose filter, followed by incubation with RbohD, RbohF, or their fragments. The filter was then incubated with anti-His antibody, followed by incubation with a second antibody conjugated with alkaline phosphatase. RbohD and RbohF proteins (or their fragments) bound to lipids on filters were visualized by staining alkaline phosphatase activity.

Liposomes were prepared according to references (Avantilipids.com; Hayes et al., 2004) with some modifications. Briefly, 16:0-18:2 PC (3.2 μ mol) and mixtures of 16:0-18:2 PC and 16:0-18:2 PA in a 3:1 molar ratio (2.4 μ mol and 0.8 μ mol, respectively) were dried under gas nitrogen. Lipid films were rehydrated in 1 mL of extrusion buffer (25 mM HEPES, pH 7.5, and 250 mM raffinose) at 42°C for 1 h and then processed by vortexing for six 30-s cycles, freezing under ethanol-dry ice mixture, and thawing under 42°C. The lipid suspension was then extruded 11 times through a polycarbonate membrane (pore size 0.2 μ m; Avanti Polar Lipids) to produce an optically clear suspension. The suspension was diluted with 3 volumes of binding buffer (25 mM HEPES, pH 7.5, 50 mM KCl, 1 mM CaCl₂, and 1 mM MgCl₂) and centrifuged at 100,000g at 20°C for 20 min. The pellet was washed once with binding buffer and then gently resuspended in 1 mL of binding buffer to obtain liposomes of 3.2 mM phospholipid. For liposome binding, the supernatants of expressed RbohD330 and RbohF341 were diluted to 0.5 μ g/ μ L, while supernatants of RbohD100 and RbohF104 were diluted to 1.25 μ g/ μ L with binding buffer. Two hundred microliters of liposome and 200 μ L diluted protein extracts were mixed and incubated at 4°C for 1 h by gentle shaking. The mixture was then centrifuged at 14,000g for 20 min to obtain a pellet. The liposome pellet was washed three times with binding buffer. The bound protein was separated on a 12% SDS-PAGE gel, transferred onto a polyvinylidene difluoride membrane, and immunoblotted with anti-His antibody conjugated with an alkaline phosphatase. The protein was made visible by staining for alkaline phosphatase activity.

The ELISA-based assay was carried out according to Ghosh et al. (1996). Phospholipids were coated on the wells of a 96-well titer plates and incubated with His-tagged RbohD or RbohF, followed by incubation with anti-His antibody and spectrometric measurements.

Protoplast Isolation, Transient Expression of Proteins, and Assaying ROS Production and NADPH Oxidase Activity

Mesophyll cell protoplasts were isolated from *Arabidopsis* leaves as described previously (Zhang et al., 2004). GCPs were isolated according to a procedure described by Pandey et al. (2002) with the following modifications. The basic solution contained 5 mM MES-Tris, pH 5.5, 0.5 mM CaCl₂, 0.5 mM MgCl₂, 10 μ M KH₂PO₄, 0.5 mM ascorbic acid (AsA), and 0.45 M sorbitol. Enzyme 1 consisted of 1% cellulase R10, 0.1% (w/v) PVP-40, 0.25% BSA, and 0.5 mM AsA, and Enzyme 2 consisted of 2.5% cellulase R10, 1.2% macerozyme R10, 0.25% BSA, and 0.5 mM AsA. After digestion, GCPs were purified using Histopaque (Sigma-Aldrich) as

described by Pandey et al. (2002). The purity of GCPs was >96% with contamination from mesophyll cell protoplasts and few chloroplasts. The GCPs were kept in basic solution on ice for 30 min before the transfection according to a procedure described previously (Zhang et al., 2004). Ten to twenty micrograms of cDNA of wild-type *RbohD*, non-PA-binding *RbohD*, and *RbohD160* and *RbohF171* (including their mutants) with HA tag was added into 100 μ L GCPs and mixed gently but well. PEG/Ca²⁺ (110 μ L; 40% PEG, v/v, 0.2 M sorbitol, and 0.1 M CaCl₂) was added to the mixture, which was mixed well, and incubated at 23°C for 5 to 30 min. After transfection, the mixture was washed twice with the basic solution and incubated at 23°C for 3 to 5 h to allow protein expression.

The protein from protoplasts was isolated according to the method of Zhang et al. (2003). Equal amounts of GCP proteins were separated by 12% SDS-PAGE gel and transferred to polyvinylidene difluoride filters. The filters were blotted with anti-HA antibody, followed by incubation with a second antibody conjugated to an alkaline phosphatase. Proteins were observed by staining for phosphatase activity.

ROS production in GCPs (or MCPs in supplemental data) was detected by DCF fluorescence (Pei et al., 2000) using a fluorescence microscope (Nikon Eclipse 800; excitation 488 nm, emission 525 nm). The fluorescence intensity was measured using Imaris 5.0.3 (Bitplane).

Total NADPH oxidase activity in protoplasts was determined using a modified assay based on the reduction of the tetrazolium dye, XTT, by superoxide radicals, O₂⁻ (Able et al., 1998). Lipids (indicated in the legends for specificity and concentration) or 10 μ M (\pm) ABA from a stock of 50 mM in 95% ethanol (final ethanol, 0.02% [v/v]) was added to GCPs (in supplemental data, MCPs). XTT (0.5 mM) was added, followed by 50 μ M NADPH to activate the reaction. After the desired time of treatment, the reaction solution was centrifuged at 200g for 30 s to pellet protoplasts. Supernatants were collected for spectrophotometric analysis of XTT formazan production at A₄₇₀. The quantity of O₂⁻ was determined using the molar extinction coefficient 2.16 \times 10⁴ M⁻¹ cm⁻¹ for XTT at 470 nm (Sutherland and Learmonth, 1997). NADPH activity was calculated according to O₂⁻ production per minute per 10⁵ cells with or without 100 units of SOD.

Isolation of the Plasma Membrane and Determination of NADPH Oxidase Activity in the Plasma Membrane

Plasma membrane vesicles were isolated from *Arabidopsis* leaves using two-phase partitioning according to a procedure described previously (Qiu et al., 2002). The membrane vesicles were resuspended in a 50 mM Tris-HCl buffer, pH 7.5, and used immediately for NADPH oxidase activity assays. A total of 1 μ M 16:0-18:2 PA, 16:0-18:2 PC, or lysoPA or 10 μ M (\pm) ABA (final ethanol, 0.02% [v/v]) was applied to the membrane vesicles (3 to 6 μ g), respectively, and incubated in the reaction buffer (50 mM Tris-HCl buffer, pH 7.5, and 0.5 mM XTT). NADPH (50 μ M) was used to initiate the reaction. After 10 min at 25°C, the reaction solution was used for spectrophotometric analysis of XTT formazan production at A₄₇₀. NADPH activity was expressed as Δ A₄₇₀ per milligram protein per minute. Δ A₄₇₀ represents the difference in XTT formazan absorbance at 470 nm in the presence and absence of 100 units of SOD.

Immunoblotting of PLD α Protein in Protoplasts

Total proteins from mesophyll cell and guard cell protoplasts were isolated according to the method of Zhang et al. (2003). PLD α immunoblotting was carried out according to previous procedures (Sang et al., 2001b).

RbohD-GFP Expression

The PCR fragments of native *RbohD-GFP* and mutated *RbohD-GFP* with the quadruple mutation R(149,150,156,157)A were cloned into the *EcoRI*

and *KpnI* restriction sites of the pCAMBIA1205 vector. Both binary plasmids were transformed into *Agrobacterium tumefaciens* (C58C1, GV3101) by electroporation. The suspension of *Agrobacterium* was then infiltrated into 4-d-old *Arabidopsis* seedlings according to a procedure described by Marion et al. (2008). The fluorescence in cotyledons was observed under a confocal microscope (Leica) after 3 d. Approximately 70 to 85% of seedlings were transformed. The cotyledons were incubated with 2 μM (\pm) ABA, 50 μM PA, or 50 μM PC for 2 h before stomatal aperture measurements.

ROS and NO Detection in Guard Cells of Epidermal Peels

ROS production in guard cells in epidermal peels was detected using DCF according to the method described by Pei et al. (2000). Epidermal peels were floated in incubation buffer (10 mM MES-KOH, pH 6.15, 10 mM KCl, 0.2 mM CaCl_2 , and 0.1 mM EGTA) for 2 h under cool white light ($150 \mu\text{mol m}^{-2} \text{s}^{-1}$) at 22°C to induce stomatal opening and then loaded with 50 μM H_2DCFDA for 10 min and washed for 20 min in an incubation buffer. ABA was added at the desired time of the treatment. Ethanol (0.1%) was added as a control experiment. Epidermal peels were observed for fluorescence using a confocal microscope (Leica), with excitation at 488 nm and emission at 525 nm.

NO level in guard cells was analyzed using an NO-sensitive dye, 4, 5-diaminofluorescein diacetate (DAF-2DA) (Sigma-Aldrich). Epidermal peels were floated in an incubation buffer under light for 2 h to induce stomatal opening and loaded with 10 μM DAF-2DA for 10 min before washing in incubation buffer for 20 min. The epidermal peels were incubated for an additional 10 min in the presence of various compounds (as indicated in the legends) before being viewed under a confocal microscope. For PTIO treatment, PTIO was applied for 30 min prior to ABA or SNP treatment. The images were observed under a confocal microscope with excitation at 488 nm and emission at 535 nm.

DCF and DAF fluorescence intensity was measured by Leica confocal software (version 2.5). Data were quantified as mean pixel intensities.

Stomatal Aperture Measurement

Stomatal aperture was measured according to the procedure described previously (Zhang et al., 2004). Briefly, epidermal peels were floated in an incubation buffer (10 mM KCl, 0.2 mM CaCl_2 , 0.1 mM EGTA, and 10 mM MES-KOH, pH 6.15). After incubation for 2.5 h under a cool white light at 23°C to induce stomatal opening, 50 μM (\pm) ABA from a stock of 50 mM in 95% ethanol (final ethanol, 0.1% [v/v]), 100 μM H_2O_2 , or 100 μM SNP was applied separately. For DPI treatment, DPI was added to an incubation buffer for 30 min before treatment. Stomatal aperture was recorded under a microscope and measured using Image J (National Institutes of Health).

ESI-MS/MS Analysis of Lipid Molecular Species

For lipid profiling, expanded leaves of 4- to 5-week-old plants were sprayed with 100 μM (\pm) ABA. The excised leaves were immersed in 3 mL of isopropanol with 0.01% butylated hydroxytoluene (75°C) immediately after sampling to terminate lipolytic activities. Lipid extraction, ESI-MS/MS analysis, and quantification were done as described previously (Devaiah et al., 2006). Five replicates of each treatment were carried out and analyzed.

Accession Numbers

Sequence data from this article can be found in the Arabidopsis Genome Initiative database under the following accession numbers: *PLD α 1*,

At3g15730; ABI1, At4g26080; *RbohD*, At5g47910; *RbohF*, At1g64060; and *Actin8*, At1g49240.

Supplemental Data

The following materials are available in the online version of this article.

Supplemental Figure 1. ROS Assay with NADPH Oxidase Inhibitor and Superoxide Donor.

Supplemental Figure 2. Vehicle Effects on ROS Production, Stomatal Closure, *RAB 18* Expression, and $\text{PLD}\alpha$ Activity.

Supplemental Figure 3. H_2O_2 Content in Wild-Type and *pld α 1* Leaves, and Effect of Applied H_2O_2 on Stomatal Closure.

Supplemental Figure 4. Sequence Alignment of *RbohD* and *RbohF* Proteins.

Supplemental Figure 5. Detection of Potential PtdInsPs Binding to *Rbohs* on Filter.

Supplemental Figure 6. PA Activation of NADPH Oxidase Activity in a Dose-Dependent Manner.

Supplemental Figure 7. Effect of di16:0 PA on ROS Production and Stomatal Closure.

Supplemental Figure 8. Phenotypes of Seedlings Transiently Expressing *RbohD*.

Supplemental Figure 9. DAB Staining for ROS in Cotyledons Transiently Expressing *RbohD*.

Supplemental Figure 10. Lipid Specificity for ROS Generation in GCPs of *pld α 1*, *rbohD*, and *rbohF*.

Supplemental Figure 11. Detecting PA Concentration-Dependent *Rboh* Binding by the ELISA Assay.

Supplemental Figure 12. Water Loss from Wild-Type and *pld α 1* Plants.

Supplemental Figure 13. *RAB18* Expression in the Wild Type, *pld α 1*, *rbohD*, and *rbohF*.

Supplemental Table 1. PCR Primers Used in This Article.

Supplemental Methods.

Supplemental References.

ACKNOWLEDGMENTS

We thank June M. Kwak (University of Maryland) and Jeffery L. Dangel (University of North Carolina) for *rboh* mutants and Yan Guo (National Institute of Biology Science, China) for GFP vector. We also thank Jiangzhe Zhao, Yakang Jin, Mary R. Roth, and Ye Lu for assistance in the experiments. The work was supported by the Chinese National Key Basic Research Project (2006CB100100), by grants from National Science Foundation of China (30625027 and 90817014) and Ministry of Education of China (B07030, 20060307019, and C-0705) to W.Z., and by grants from National Science Foundation (IOS-0818740) and the USDA (2007-35318-18393) to X.W. Lipidomic analysis development and instrument acquisition at Kansas Lipidomics Research Center was supported by the National Science Foundation (EPS 0236913, MCB 0455318, and DBI 0521587), Kansas Technology Enterprise Corporation, K-IDEA Networks of Biomedical Research Excellence of National Institutes of Health (P20RR16475), and Kansas State University.

Received September 1, 2008; revised July 21, 2009; accepted July 31, 2009; published August 18, 2009.

REFERENCES

- Able, A.J., Guest, D.I., and Sutherland, M.W. (1998). Use of a new tetrazolium-based assay to study the production of superoxide radicals by tobacco cell cultures challenged with avirulent zoospores of *Phytophthora parasitica* var *nicotianae*. *Plant Physiol.* **117**: 491–499.
- Ago, T., Kuiibayashi, F., Hiroaki, H., Takeya, R., Ito, T., and Kohda, D. (2003). Phosphorylation of p47^{phox} directs phox homology domain from SH3 domain toward phosphoinositides, leading to phagocyte NADPH oxidase activation. *Proc. Natl. Acad. Sci. USA* **100**: 4474–4479.
- An, Z., Jing, W., Liu, Y., and Zhang, W. (2008). Hydrogen peroxide generated by copper amine oxidase is involved in abscisic acid-induced stomatal closure in *Vicia faba*. *J. Exp. Bot.* **59**: 815–825.
- Asai, S., Ohta, K., and Yoshioka, H. (2008). MAPK signaling regulates nitric oxide and NADPH oxidase-dependent oxidative bursts in *Nicotiana benthamiana*. *Plant Cell* **20**: 1390–1406.
- Assmann, S.M. (2003). OPEN STOMATA1 opens the door to ABA signaling in *Arabidopsis* guard cells. *Trends Plant Sci.* **8**: 151–153.
- Babior, B.M. (2004). NADPH oxidase. *Curr. Opin. Immunol.* **16**: 42–47.
- Bargmann, B.O., and Munnik, T. (2005). The role phospholipase D in plant stress responses. *Curr. Opin. Plant Biol.* **9**: 515–522.
- Bright, J., Desikan, R., Hancock, J.T., Weir, I.S., and Neill, S.J. (2006). ABA-induced NO generation and stomatal closure in *Arabidopsis* are dependent on H₂O₂ synthesis. *Plant J.* **45**: 113–122.
- Coursol, S., Fan, L.-M., Le Stunff, H., Splegel, S., Gilroy, S., and Assmann, S.M. (2003). Sphingolipid signaling in *Arabidopsis* guard cells involves heterotrimeric G proteins. *Nature* **423**: 651–654.
- de Jong, C.F., Laxalt, A.M., Bargmann, B.O.R., De Wit, P.J.G.M., Joosten, M.H.A.J., and Munnik, T. (2004). Phosphatidic acid accumulation is an early response in the *Cf-4/Avr4* interaction. *Plant J.* **39**: 1–12.
- Desikan, R., Cheung, M.-K., Bright, J., Henson, D., Hancock, J.T., and Neill, S.J. (2004). ABA, hydrogen peroxide and nitric oxide signaling in stomatal guard cells. *J. Exp. Bot.* **55**: 205–212.
- Desikan, R., Griffiths, R., Hancock, J., and Neill, S.J. (2002). A new role for old enzyme: Nitrate reductase-mediated nitric oxide generation is required for abscisic acid-induced stomatal closure in *Arabidopsis thaliana*. *Proc. Natl. Acad. Sci. USA* **99**: 16314–16318.
- Devaiah, S.P., Roth, M.R., Baughman, E., Li, M., Tamura, P., Jeannotte, R., Welti, R., and Wang, X. (2006). Quantitative profiling of polar glycerolipid species and the role of phospholipase Dα1 in defining the lipid species in *Arabidopsis* tissues. *Phytochemistry* **67**: 1907–1924.
- Fan, L.-M., Zhao, Z., and Assmann, S.M. (2004). Guard cells: A dynamic signaling model. *Curr. Opin. Plant Biol.* **7**: 537–546.
- Finkelstein, R.R., Gampala, S.S., and Rock, C.D. (2002). Abscisic acid signaling in seeds and seedlings. *Plant Cell* **14**: S15–S45.
- Foreman, J., Demidchik, V., Bothwell, J.H.F., Mylona, P., Miedema, H., Torres, M.A., Linstead, P., Costa, S., Brownlee, C., Jones, J.D.G., Davies, J.M., and Dolan, L. (2003). Reactive oxygen species produced by NADPH oxidase regulated plant cell growth. *Nature* **422**: 442–446.
- Garcia-Mata, C., Gay, R., Sokolovski, S., Hills, A., Lamattina, L., and Blatt, M.R. (2003). Nitric oxide regulates K⁺ and Cl⁻ channels in guard cells through a subset of abscisic acid-evoked signaling pathways. *Proc. Natl. Acad. Sci. USA* **100**: 11116–11121.
- Ghosh, S., Strum, J.C., Sciorra, V.A., Danniell, L., and Bell, R.M. (1996). Raf-1 kinase possesses distinct binding domains for phosphatidylserine and phosphatidic acid. *J. Biol. Chem.* **271**: 8472–8480.
- Gómez-Merino, F.C., Arana-Ceballos, F.A., Trejo-Téllez, L.I., Skirycz, A., Brearley, C.A., Dörmann, P., and Mueller-Roeber, B. (2005). *Arabidopsis* AtDGK7, the smallest member of plant diacylglycerol kinases (DGKs), displays unique biochemical features and saturates at low substrate concentration. *J. Biol. Chem.* **280**: 34888–34899.
- Gosti, F., Beaudoin, N., Serizet, C., Webb, A.A.R., Vartanian, N., and Giraudat, J. (1999). ABI1 protein phosphatase 2C is a negative regulator of abscisic acid signaling. *Plant Cell* **11**: 1897–1909.
- Groom, Q.J., Torres, M.A., Fordham-Skelton, A.P., Hammond-Kosack, K.E., Robinson, N.J., and Jones, J.D.G. (1996). *rbohA*, a rice homologue of the mammalian gp91^{phox} respiratory burst oxidase gene. *Plant J.* **10**: 515–522.
- Hancock, J.F. (2007). PA promoted to manager. *Nat. Cell Biol.* **9**: 615–617.
- Hayes, M.J., Merrifield, C.J., Shao, D., Ayala-Sanmartin, J., Schorey, C.D., Levine, T.P., Proust, J., Curran, J., Bailly, M., and Moss, S.E. (2004). Annexin 2 binding to phosphatidylinositol 4,5-bisphosphate on endocytic vesicles is regulated by the stress response pathway. *J. Biol. Chem.* **279**: 14157–14164.
- Heyworth, P.G., Bohl, B.P., Bokoch, G.M., and Curnutte, J.T. (1994). Rac translocates independently of the neutrophil NADPH oxidase components p47^{phox} and p67^{phox}. Evidence for its interaction with flavocytochrome b₅₅₈. *J. Biol. Chem.* **269**: 30749–30752.
- Heyworth, P.G., Curnutte, J.T., Nauseef, W.M., Volpp, B.D., Pearson, D.W., Rosen, H., and Clark, R.A. (1991). Neutrophil nicotinamide adenine dinucleotide phosphate oxidase assembly. Translocation of p47^{phox} and p67^{phox} requires interaction between p47^{phox} and cytochrome b₅₅₈. *J. Clin. Invest.* **87**: 352–356.
- Himmelbach, A., Hoffmann, T., Leube, M., Höhener, B., and Grill, E. (2002). Homeodomain protein ATHB6 is a target of the protein phosphatase ABI1 and regulates hormone responses in *Arabidopsis*. *EMBO J.* **21**: 3029–3038.
- Hirayama, T., and Shinozaki, K. (2007). Perception and transduction of abscisic acid signals: Keys to the function of the versatile plant hormone ABA. *Trends Plant Sci.* **12**: 343–351.
- Honbou, K., Minakami, R., Yuzawa, S., Takeya, R., Suzuki, N.N., Kamakura, S., Sumimoto, H., and Inagaki, F. (2007). Full-length p40^{phox} structure suggests a basis for regulation mechanism of its membrane binding. *EMBO J.* **26**: 1176–1186.
- Jacob, T., Ritchie, S., Assmann, S.M., and Gilroy, S. (1999). Abscisic acid signal transduction in guard cells is mediated by phospholipase D activity. *Proc. Natl. Acad. Sci. USA* **96**: 12192–12197.
- Kami, K., Takeya, R., Sumimoto, H., and Kohda, D. (2002). Diverse recognition of non-PxxP peptide ligands by the SH3 domains from p67^{phox}, Grb2 and Pex13p. *EMBO J.* **21**: 4268–4276.
- Kanai, F., Liu, H., Field, S.J., Akbary, H., Matsuo, T., Brown, G.E., Cantley, L.C., and Yaffe, M.B. (2001). The PX domains of p47^{phox} and p40^{phox} bind to lipid products of PI(3). *Nat. Cell Biol.* **3**: 675–678.
- Karathanassis, D., Stahelin, R.V., Bravo, J., Perisic, O., Pacold, C.M., Cho, W., and Williams, R.L. (2002). Binding of the PX domain of p47^{phox} to phosphatidylinositol 3,4-bisphosphate and phosphatidic acid is masked by an intramolecular interaction. *EMBO J.* **21**: 5057–5068.
- Kawasaki, T., Henmi, K., Ono, E., Hatakeyama, S., Iwano, M., Satoh, H., and Shimamoto, K. (1999). The small GTP-binding protein rac is a regulator of cell death in plants. *Proc. Natl. Acad. Sci. USA* **96**: 10922–10926.
- Keller, T., Damude, H.G., Wener, D., Doerner, P., Dixon, R.A., and Lamb, C. (1998). A plant homolog of the neutrophil NADPH oxidase gp91^{phox} subunit gene encodes a plasma membrane protein with Ca²⁺ binding motifs. *Plant Cell* **10**: 255–266.
- Kobayashi, M., Ohura, I., Kawakita, K., Yokota, N., Fujiwara, M., Shimamoto, K., Doke, N., and Yoshioka, H. (2007). Calcium-dependent protein kinases regulate the production of reactive oxygen species by potato NADPH oxidase. *Plant Cell* **19**: 1065–1080.

- Köhler, B., Hills, A., and Blatt, M.R.** (2003). Control of guard cell ion channels by hydrogen peroxide and abscisic acid indicates their action through alternate signaling pathways. *Plant Physiol.* **131**: 385–388.
- Kwak, J.M., Mori, I.C., Pei, Z.-M., Leonhardt, N., Torres, M.A., Dangl, J.L., Bloom, R.E., Boddle, S., Jones, J.D.G., and Schroeder, J.I.** (2003). NADPH oxidase *AtrbohD* and *AtrbohF* genes function in ROS-dependent ABA signaling in *Arabidopsis*. *EMBO J.* **22**: 2623–2633.
- Kwak, J.M., Nguyen, V., and Schroeder, J.I.** (2006). The role of reactive oxygen species in hormonal responses. *Plant Physiol.* **141**: 323–329.
- Lanteri, M.L., Laxalt, A.M., and Lamattina, L.** (2008). Nitric oxide triggers phosphatidic acid accumulation via phospholipase D during auxin-induced adventitious root formation in cucumber. *Plant Physiol.* **147**: 188–198.
- Laxalt, A.M., Raho, N., ten Have, A., and Lamattina, L.** (2007). Nitric oxide is critical for inducing phosphatidic acid accumulation in xylanase-elicited tomato cells. *J. Biol. Chem.* **282**: 21160–21168.
- Lee, Y., Bak, G., Chuang, W.-I., Cho, H.-T., and Lee, Y.** (2008). Roles of phosphatidylinositol 3-kinase in root hair growth. *Plant Physiol.* **147**: 624–635.
- Leshem, Y., Seri, L., and Levine, A.** (2007). Induction of phosphatidylinositol 3-kinase-mediated endocytosis by salt leads to intracellular production of reactive oxygen species and salt tolerance. *Plant J.* **51**: 185–197.
- Li, S., Assmann, S.M., and Albert, R.** (2006). Predicting essential components of signal transduction network: A dynamic model of guard cell abscisic acid signaling. *PLoS Biol.* **4**: 1732–1748.
- Liu, X.G., Yue, Y.L., Li, B., Nie, Y.L., Li, W., Wu, W.H., and Ma, L.G.** (2007). A G protein-coupled receptor is a plasma membrane receptor for the plant hormone abscisic acid. *Science* **315**: 1712–1716.
- Ma, Y., Szostkiewicz, I., Krote, A., Moes, D., Yang, Y., Christmann, A., and Grill, E.** (2009). Regulators of PP2C phosphatase activity function as abscisic acid sensors. *Science* **324**: 1064–1068.
- Marion, J., Bach, L., Bellec, Y., Meyer, C., Gissot, L., and Faure, J.D.** (2008). Systematic analysis of protein subcellular localization and interaction using high-throughput transient transformation of *Arabidopsis* seedlings. *Plant J.* **56**: 169–179.
- Meinhard, M., and Grill, E.** (2001). Hydrogen peroxide is a regulator of ABI1, a protein phosphatase 2C from *Arabidopsis*. *FEBS Lett.* **508**: 443–446.
- Meinhard, M., Rodríguez, P.L., and Grill, E.** (2002). The sensitivity of ABI2 to hydrogen peroxide links the abscisic acid-response regulator to redox signalling. *Planta* **214**: 775–782.
- Merlot, S., Gosti, F., Guerrier, D., Vavasseur, A., and Giraudat, J.** (2001). The ABI1 and ABI2 protein phosphatases 2C act in a negative feedback regulatory loop of the abscisic acid signalling pathway. *Plant J.* **25**: 295–303.
- Mishra, G., Zhang, W., Deng, F., and Wang, X.** (2006). A bifurcating pathway directs abscisic acid effects on stomatal closure and opening in *Arabidopsis*. *Science* **312**: 264–266.
- Morel, J., Fromentin, J., Blein, J.P., Simon-Plas, F., and Elmayan, T.** (2004). Rac regulation of *NtrbohD*, the oxidase responsible for the oxidative burst in elicited tobacco cell. *Plant J.* **37**: 282–293.
- Munnik, T., and Testerink, C.** (2009). Plant phospholipid signaling – In a nutshell. *J. Lipid Res.* **50**: S260–S265.
- Neill, S., Barros, R., Bright, J., Desikan, R., Hancock, J., Harrison, J., Morris, P., Ribeiro, D., and Wilson, I.** (2008). Nitric oxide, stomatal closure, and abiotic stress. *J. Exp. Bot.* **59**: 165–176.
- Nilson, S.E., and Assmann, S.M.** (2007). The control of transpiration. Insights from *Arabidopsis*. *Plant Physiol.* **143**: 19–27.
- Nuhse, T.S., Bottrill, A.R., Jones, A.M., and Peck, S.C.** (2007). Quantitative phosphoproteomic analysis of plasma membrane proteins reveals regulatory mechanisms of plant innate immune responses. *Plant J.* **51**: 931–940.
- Ogasawara, Y., et al.** (2008). Synergistic activation of the *Arabidopsis* NADPH oxidase *AtrbohD* by Ca^{2+} and phosphorylation. *J. Biol. Chem.* **283**: 8885–8892.
- Ono, E., Wong, H.L., Kawasaki, T., Hasegawa, M., Kodama, O., and Shimamoto, K.** (2001). Essential role of the small GTPase Rac in disease resistance of rice. *Proc. Natl. Acad. Sci. USA* **98**: 759–764.
- Pandey, S., Nelson, D.C., and Assmann, S.M.** (2009). Two novel GPCR-type G proteins are abscisic acid receptors in *Arabidopsis*. *Cell* **136**: 136–148.
- Pandey, S., Wang, X.-Q., Coursol, S.A., and Assmann, S.M.** (2002). Preparation and applications of *Arabidopsis thaliana* guard cell protoplasts. *New Phytol.* **153**: 517–526.
- Park, J., Gu, Y., Lee, Y., Yang, Z., and Lee, Y.** (2004). Phosphatidic acid induces leaf cell death in *Arabidopsis* by activating the Rho-related small G protein GTPase-mediated pathway of reactive oxygen species generation. *Plant Physiol.* **134**: 129–136.
- Park, K.-Y., Jung, J.-Y., Park, J., Hwang, J.-U., Kim, Y.-W., Hwang, I., and Lee, Y.A.** (2003). Role for phosphatidylinositol 3-phosphate in abscisic acid-induced reactive oxygen species generation in guard cells. *Plant Physiol.* **132**: 92–98.
- Park, S.-Y., et al.** (2009). Abscisic acid inhibits type 2C protein phosphatases via the PRY/PYL family of START proteins. *Science* **324**: 1068–1071.
- Pei, Z.-M., Murata, Y., Benning, G., Thomine, S., Klüsener, B., Allen, G.J., Grill, E., and Schroeder, J.I.** (2000). Calcium channels activated by hydrogen peroxide mediate abscisic acid signalling in guard cells. *Nature* **406**: 731–734.
- Perera, I.Y., Hung, C.-Y., Moore, C.D., Stevenson-Paulik, J., and Boss, W.J.** (2008). Transgenic *Arabidopsis* plants expressing the type 1 inositol 5-p-phosphatase exhibit increased drought tolerance and altered abscisic acid signaling. *Plant Cell* **20**: 2876–2893.
- Piomelli, D., Astarita, G., and Rapaka, R.** (2007). A neuroscientist's guide to lipidomics. *Nat. Rev. Neurosci.* **8**: 743–754.
- Qiu, Q.-S., Guo, Y., Dietrich, M.A., Schumaker, K.S., and Zhu, J.-K.** (2002). Regulation of SOS1, a plasma membrane Na^+/H^+ exchanger in *Arabidopsis thaliana*, by SOS2 and SOS3. *Proc. Natl. Acad. Sci. USA* **99**: 8436–8441.
- Sang, Y., Cui, D., and Wang, X.** (2001a). Phospholipase D and phosphatidic acid-mediated generation of superoxide in *Arabidopsis*. *Plant Physiol.* **126**: 1449–1458.
- Sang, Y., Zheng, S., Li, W., Huang, B., and Wang, X.** (2001b). Regulation of plant water loss by manipulating the expression of phospholipase D α . *Plant J.* **28**: 135–144.
- Schroeder, J.I., Kwak, J.M., and Allen, G.J.** (2001). Guard cell abscisic acid signalling and engineering drought hardiness in plants. *Nature* **410**: 327–330.
- Schultheiss, H., Dechert, C., Kogel, K.H., and Huckelhoven, R.** (2002). A small GTP-binding host protein is required for entry of powdery mildew fungus into epidermal cells of barley. *Plant Physiol.* **128**: 1447–1454.
- Shen, Y.Y., et al.** (2006). The Mg-chelatase H subunit is an abscisic acid receptor. *Nature* **443**: 823–826.
- Sokolovski, S., and Blatt, M.R.** (2004). Nitric oxide block of outward-rectifying K^+ channels indicates direct control by protein nitrosylation in guard cells. *Plant Physiol.* **136**: 4275–4284.
- Suharsono, U., Fujisawa, Y., Kawasaki, T., Iwasaki, Y., Satoh, H., and Shimamoto, K.** (2002). The heterotrimeric G protein α subunit acts upstream of the small GTPase Rac in disease resistance of rice. *Proc. Natl. Acad. Sci. USA* **99**: 13307–13312.
- Suhita, D., Raghavendra, A.S., Kwak, J.M., and Vavasseur, A.** (2004). Cytoplasmic alkalization precedes reactive oxygen species production

- during methyl jasmonate- and abscisic acid- induced stomatal closure. *Plant Physiol.* **134**: 1536–1545.
- Sutherland, M.W., and Learmonth, B.A.** (1997). The tetrazolium dyes MTS and XTT provide new quantitative assays for superoxide and superoxide dismutase. *Free Radic. Res.* **27**: 283–289.
- Testerink, C., and Munnik, T.** (2005). Phosphatidic acid: A multifunctional stress signaling lipid in plants. *Trends Plant Sci.* **10**: 368–375.
- Torres, M.A., and Dangl, J.L.** (2005). Functions of the respiratory burst oxidase in biotic interactions, abiotic stress and development. *Curr. Opin. Plant Biol.* **8**: 397–403.
- Torres, M.A., Dangl, J.L., and Jones, J.D.G.** (2002). *Arabidopsis* gp91^{phox} homologues AtrbohD and AtrbohF are required for accumulation of reactive oxygen intermediates in the plant defense response. *Proc. Natl. Acad. Sci. USA* **99**: 523–528.
- Torres, M.A., Onouchi, H., Hamada, S., Machida, C., Hammond-Kosack, K.E., and Jones, J.D.G.** (1998). Six *Arabidopsis thaliana* homologues of the human respiratory burst oxidase (gp91^{phox}). *Plant J.* **14**: 365–370.
- Wang, H., and Joseph, J.A.** (1999). Quantifying cellular oxidative stress by dichlorofluorescein assay using microplate reader. *Free Radic. Biol. Med.* **27**: 612–616.
- Wang, X.** (2005). Regulatory functions of phospholipase D and phosphatidic acid in plant growth, development, and stress responses. *Plant Physiol.* **139**: 566–573.
- Wang, X., Devaiah, S.P., Zhang, W., and Welti, R.** (2006). Signaling functions of phosphatidic acid. *Prog. Lipid Res.* **45**: 250–278.
- Wang, X.-Q., Ullah, H., Jones, A.M., and Assmann, S.M.** (2001). G protein regulation of ion channels and abscisic acid signaling in *Arabidopsis* guard cell. *Science* **292**: 2070–2072.
- Wong, H.L., Pinontoan, R., Hayashi, K., Tabata, R., Yaeno, T., Hasegawa, K., Kojima, C., Yoshioka, H., Iba, K., Kawasaki, T., and Shimamoto, K.** (2007). Regulation of rice NADPH oxidase by binding of Rac GTPase to its N-terminal extension. *Plant Cell* **19**: 4022–4034.
- Xiong, L., and Zhu, J.-K.** (2003). Regulation of abscisic acid biosynthesis. *Plant Physiol.* **133**: 29–36.
- Yoshioka, H., Numata, N., Nakajima, K., Katou, S., Kawakita, K., Rowland, O., Jones, J.D., and Doke, N.** (2003). *Nicotiana benthamiana* gp91^{phox} homologs NbrbohA and NbrbohB participate in H₂O₂ accumulation and resistance to *Phytophthora infestans*. *Plant Cell* **15**: 706–718.
- Zhang, W., Qin, C., Zhao, J., and Wang, X.** (2004). Phospholipase D α 1-derived phosphatidic acid interacts with ABI1 phosphatase 2C and regulates abscisic acid signaling. *Proc. Natl. Acad. Sci. USA* **101**: 9508–9513.
- Zhang, W., Wang, C., Qin, C., Wood, T., Olafsdottir, G., Welti, R., and Wang, X.** (2003). The oleate-stimulated phospholipase D, PLD δ , and phosphatidic acid decrease H₂O₂-induced cell death in *Arabidopsis*. *Plant Cell* **15**: 2285–2295.
- Zhang, W., Yu, L., Zhang, Y., and Wang, X.** (2005). Phospholipase D in the signaling networks of plant response to abscisic acid and reactive oxygen species. *Biochim. Biophys. Acta* **1736**: 1–9.